A thesis on

# Role of deformations in decay of $^{196}$Pt formed in $^{132}$Sn+$^{64}$Ni reaction

Thesis submitted in partial fulfillment of the requirement for
The award of the degree of
Masters of Science
In
PHYSICS

Under
the supervsion of
Dr.Manoj Sharma

Submitted by
Shweta Rani
Roll no. - 30704018

School of physics and Material Science
Thapar University
Patiala – 147004 (PUNJAB)
INDIA

# CERTIFICATE

This is to certify that Ms. Shweta Rani, Roll No. 30704018 has worked on this thesis report as a partial fulfillment for award of the degree of MASTERS OF SCIENCE in physics. I certify that the matter embodied in this report is of candidate's own record and not submitted to any other university in any part or full form for the award of such a degree.

9/7/09

(Dr. Manoj K Sharma)
*Supervisor*
SPMS, Thapar University
Patiala

Countersigned by:

9/7/09

Dr. O.P. Pandey
(Prof. & Head)
School of Physics and Materials Science
**Thapar University, Patiala.**

13/7/09

Dr. R.K. Sharma
Dean of academic Affairs
Thapar University
**Patiala.**

## Acknowledgement

I owe my deepest gratitude to **Dr. Manoj Sharma**, *my worthy supervisor*, who has been an inspiration during my research work. Without him, this dissertation would not have been possible. I thank him for his patience and encouragement that carried me on through difficult times, and for his insights and suggestions that helped to shape my research skills. I express my sincere thanks to him for his valuable guidance in carrying out work under his effective supervision, encouragement and cooperation. His visionary thoughts have influenced me greatly. His dynamical attitude has empowered me with zeal of energy to conquer the minor details of my research work.

I also thank **Dr. O. P. Pandey**, Professor and Head, School of Physics and Material Science for his support and providing facilities.

A special word of thanks to **Mrs. Shefali Kanwar**, Research Scholars for the help and valuable suggestions whenever I needed out of her busy schedule.

Special thanks to all my friends and the staff at the School of Physics and Material Sciences for providing me a friendly atmosphere and encouraging me throughout this work. Their assistance and partnership were of great pleasure. I am deeply thankful to my Family, their moral support and patience has bared fruit through completion of this Thesis.

Shweta Rani

Shweta Rani

Roll no. 30704018

Date: 9 July, 2009

## Abstract

In view of present day developments in the domain of nuclear physics, it is extremely important & essential to study the nuclear properties and related issues at the extreme conditions of temperature, angular momentum & energies in order to respond the exotic experimentations being conducted & planned in near future. In order to meet such challenges, it becomes extremely essential to update the standard of theoretical computations & as to make meaningful predictions in the related field. It is therefore important to account for the shapes of larger projectile combinations by considering proper deformation & orientation effects.

Keeping this in mind, we have investigated the role of deformations & orientation in order to understand nuclear reactions dynamics of $^{196}$Pt formed in $^{132}$Sn+$^{64}$Ni. It is reported in literature that the inclusion of deformations & orientations effects change the barrier position & barrier height significantly so as to influence the nuclear decay probabilities. It is relevant to mention here that with the inclusion of such effects barrier becomes broaden and its height gets reduced. As a consequence of this, the fusion probability gets greatly reduced.

For the present study, I have used DCM which is a very vibrant model to account for nuclear dynamics in general & nuclear structure in particular. Our calculations clearly indicate that the inclusion of deformations & orientations effects is extremely important to account for the behavior of a nuclear system.

# TABLE OF CONTENTS

# List of figures

# Chapter 1

## 1.1 INTRODUCTION

Nuclear shapes are indeed exteremly useful to understand nuclear dynamics and the quest regarding shapes of nucleus fascinated scientists for many years. Although many nuclei are spherical, but majority of them exhibit essentially not just one shape, but different shapes ranging from doorknobs to cigars. Scientists now are exploring even more exotic shapes, e.g. banana-like (referred to as "super deformation"). Such weird objects can be found, perhaps, as we approach the point where a particular collection of neutrons and protons in the nucleus becomes unstable and can exist only briefly.

Across the limits of stability we observe some very unusual phenomena. We already know that a few nuclei display a different distribution pattern for their neutrons as compared to that of protons. Although it is not entirely clear why this happens, and we need more examples and studies to explore these strange possibilities. In other words, in addition to nuclear shapes, deformations and orientation etc, the charge dependence of nuclear forces needs to be addressed carefully.

Historically, speaking, the shape of nucleus was first investigated by schuller & Schmidt by determination of nuclear electric quadrupole moment from hyperfine structure in atomic spectra. The nuclear electric quadrupole moment measures the deviation of charge distribution from a spherical shape and hence provides information about nuclear shape. The measurement of quadruple moments involves interaction of nuclear charge distribution with static charge distributions of the electrons in atomic or molecular systems or with a specified external applied electric field. Similarly, the magnetic moment of the nucleus emerges due to the magnetic field arising in the nucleus because of spin and angular momentum.

## *1.2 Nuclear Shapes*

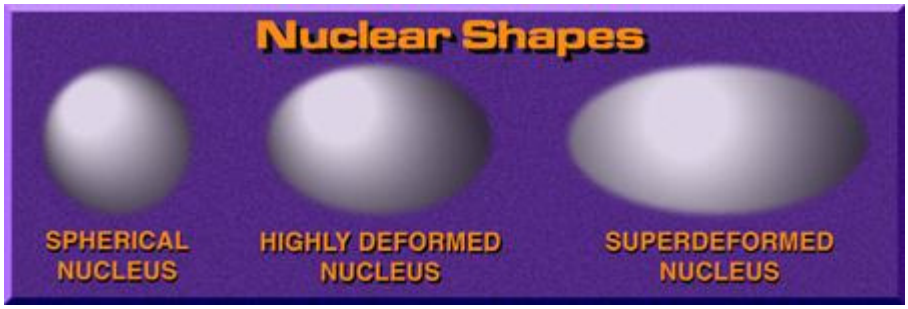


Figure 1.1. Nuclear shapes.

*A nucleus is made up of protons (positively charged particles) and neutrons (particles with no net electric charge). In a nucleus, protons and neutrons can arrange themselves in many different ways. Most commonly, the protons and neutrons each form a series of concentric shells to give the nucleus a spherical or near-spherical shape (left part of Fig.1.1). However, in some nuclei the outermost neutrons and protons move with respect to the inner protons and neutrons and the result is a "highly deformed" shape (center part of Fig.1.1), in which the length is about 1.5 times greater than its width. In even more extreme cases, "superdeformed nuclei" can result (right part of fig.1.1); with length width ratio of about 2:1*

A nucleus with a completely filled shell of either protons or neutrons is said to be magic because it is relatively more stable than nuclei with either a larger or a smaller number of nucleons. Most of magic nuclei are spherical in shape, but some nuclei can lower their energy somewhat, and hence increase their stability, by rearranging their protons and neutrons into deformed shells accommodating a different number of nucleons.These deformed shells extend possibiltity of certain deformed magic nuclei as well.

By use of theories that reproduce the magic numbers and other properties of known nuclei, theoretitians have predicted that the next spherical proton magic number is among 114/120/126 and that the next spherical neutron magic number is 184. in addition, they have predicted a deformed proton magic number at 110 and a deformed neutron magic number at 162. These predictions are made by solving the schrodinger

equation of quantum mechanics with an appropriate single particle potential to describe the motion of the proton and neutrons besides a large number of statistical models.

In many respects spherical nuclei are exceptional, as the vast majority of nuclei are deformed . Many nuclei are only slightly non-spherical, and so can still be well described by spherical nuclear models. However, for nuclei with a mass number *A*=150-200 deformation become significant and can no longer be ignored for majority of nuclei in the mass region. Hence deformation and orientation contributions become extremely important & need to be incorporated explicitly in order to account for nuclear dynamics.

So in general, the nucleus is considered to have spherical shape, but if the distribution of charges in the nucleus is not spherically symmetric , the nucleus will have quadruple moment. Quadrupole moment measures the departure of nucleus from its spherical symmetry. A nuclear quadrupole moment interacts with orbital electrons of the atom and consequently , there is a shift in atomic energy levels which lead to the hyperfine splitting of spectral lines. Due to this, deviations from spherical symmetry do occur in nuclei whose spin quantum numbers are one or more. Such nuclei may be prolate or oblate ellipsoidal. Nuclei with positive quadruple moment are prolate deformed while those with negative quadruple moment correspond to oblate deformed shapes. The quadrupole moment of a spherically symmetric nucleus is zero.

## *1.3 Quadrupole deformation*

A quadrupole deformed nucleus has a prolate or oblate ellipsoidal shape. This is the lowest order deformation seen in nuclei. A prolate ellipsoid has two equal, short axes and a single long axis; an oblate ellipsoid has two equal long axes and a single short axis. Both cases are illustrated in fig.1.2. For deformed nuclei, the axis of unequal length is often termed as deformation axis.

## 1.4 Deformation parameters

The degree to which a nucleus is deformed is described by a deformation parameter: $\varepsilon$ or β. $\varepsilon$ is the deformation neck length parameter used in the Nilsson model for describing single particle properties of the nucleus, while β is used when describing collective behaviour such as rotation [1]. In each case, a positive deformation parameter indicates a prolate shape while a negative deformation parameter describes an oblate shape.

If quadrupole moment is denoted by $\beta_2$ then the general formula for quadrupole moment is given by

$$\beta_2=2/5\ Z(b^2-a^2)$$

where Z is the atomic number of the nuclei and b and a are the semi major and semi minor axis of the nuclei.

The shape of an atomic nucleus reflects the shell structure of the protons and neutrons of which it is formed. If the shells are completely filled, we speak of a “magic” nucleus, which is spherical in shape. Most nuclei, however, tend to be deformed because their shells are only partially filled. The most commonly encountered shapes are elongated (prolate) or flattened (oblate); these shapes can change from one nucleus to its neighbour by adding or removing a proton or neutron. In some cases it is sufficient to rearrange the protons or neutrons within the same nucleus to change its shape. The same nucleus can therefore assume different shapes corresponding to states of different energy. If such states come close in energy (one thousandth of the binding energy of the nucleus or so), the different shapes can mix. According to the laws of quantum mechanics, the nucleus can coexist in different shapes (e.g. elongated and flattened) at the same time.

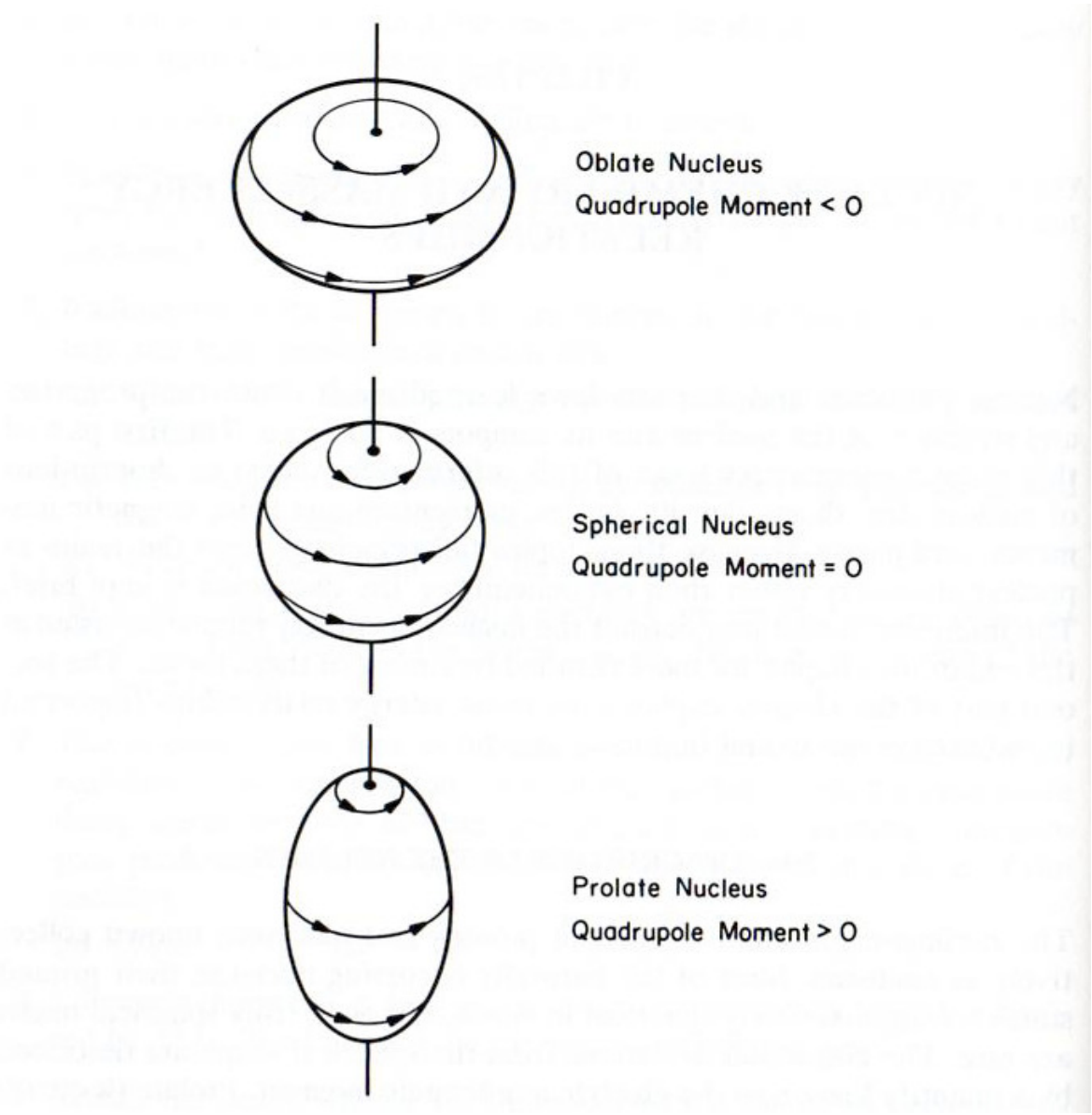


*Figure.1.2. Shapes of the nucleus. All even-Z,even-N nuclei are approximatey spherical in their ground states. Nuclei with odd Z and /or N have shapes that are spheroidal in their ground states. The deformation is indicated by the quadrouple moment of the nucleus. A negative quadrupole moment signifies a shape similar to a flattened spinning toy top(an oblate spheroid). A positive quadrupole moment is associated with a cigar shaped spheroid spinning around its long axis.(a prolate spheroid)*

In simplest form, most deformed nuclei can be approximated as quadrupole deformed (i.e. a prolate or oblate ellipsoid). However other deformations, such as octupole and hexadecapole are also important and contribute in form of tri axial deformations.

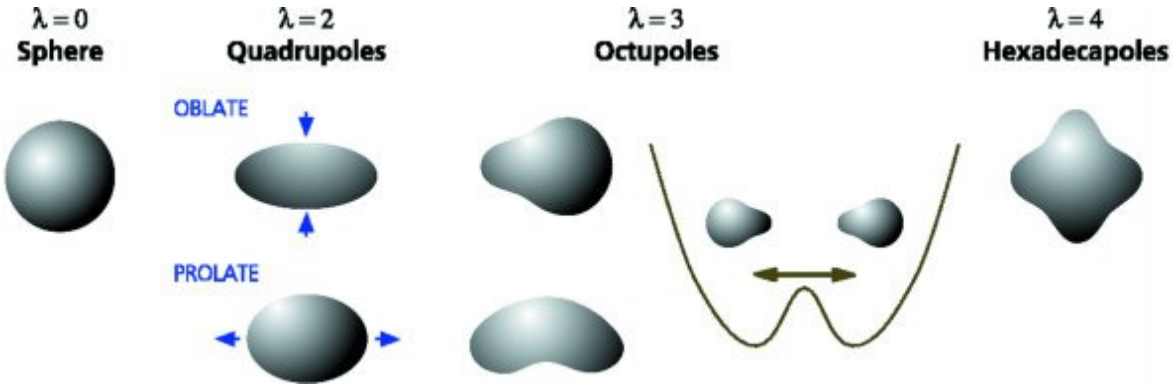


Figure 1.3. Nuclear shapes for spherical, quadrupole, octupole &hexadecapole deformations.

The contribution of higher mode deformations and choice of appropriate deformations lead to inomorous exotic shapes which in turn are emmensely useful to understand the nuclear dynamics at extreme conditions and therefore provide an important information for future experiments.

A nucleus will prefer a deformed shape rather than a spherical shape in majority of cases where deformed configurations lead to relatively less energy or more stability zone. The majority of quadrupole deformed nuclei are prolate rather than oblate deformed in their ground state[2]. This can be understood by considering two details of the single-particle levels calculated using the Nilsson model.

1. Firstly, the angular momentum of single particle states tends to be high just above shell gaps, where prolate deformation is common. This means these levels will split into many different levels when the nucleus becomes deformed, so the behaviour of these states is significant.
2. Secondly, the energy spacing between levels (with different angular momentum projections Ω) in a deformed nucleus is proportional to Ω i.e small Ω levels are closely spaced, while large Ω levels are widely spaced[2].

In case of prolate nuclei large number of orbitals occupy low energy region i.e correspond to low Ω levels where as case is reverse for oblate configurations. So one can clearly establish the fact regarding abundance of prolate shapes. This result is illustrated in fig.1.4. With more energetically favourable states possible for prolate nuclei, a nucleus is more likely to be prolate deformed.

### Prolate vs. Oblate deformation

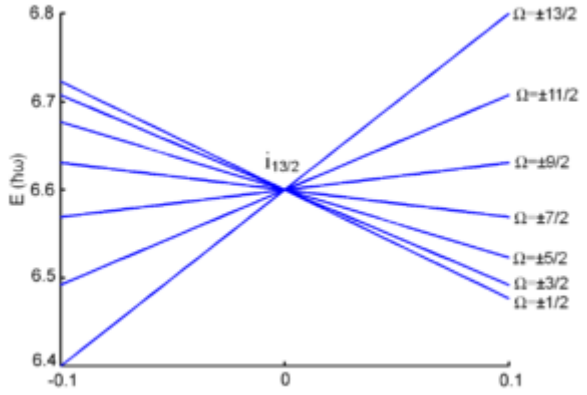


Figure1. 4

Ω-splitting for an $i_{13/2}$ orbital. More low energy levels occur on the prolate side (ε>0) than the oblate side (ε<0).[2].

## 1.5 Deformation and orientation effects of nuclei

Nuclei can be both spherical and deformed in their ground state. The shape of both nuclei participating in a reaction affects the barrier height and the potential of their interaction. The barrier height is of great importance for the reactions of subbarrier fusion and synthesis of superheavy elements. Nuclear reactions, where deformed nuclei are engaged, are widely applied to the synthesis of superheavy elements in many laboratories around the world . The reactions of subbarrier fusion of strongly deformed F, Ne, and Mg isotopes play a very important role in the burning of stars and govern their evolution. Therefore, it is important to study the properties of the interaction potential between two deformed nuclei. Beside this proper choice of orientation of target and projectile contribute emmensly and therefore need to be

handled with care. In other words; where ever a deformed configuration is considered.The orientational behaviour of nuclear systems cannot be ignored.

The depth and the width of the capture well in the nucleus-nucleus interaction potential, as well as the barrier height, are known to play a dominant role in the formation of a compound nucleus in fusion-fission reaction .This feature is associated with the necessity to overcome the barrier that exists between two separated nuclei and with a formation of a scission neck between contacting nuclei in the capture well, as well as with the evolution of shape of the nuclear system .Therefore, it is very important to study the influence of deformation and an orientations on the nucleus-nucleus interaction potential.

In the fusion of deformed and relatively oriented nuclei the distance between mass centers of the massive reactants rely on the orientation of the deformed nuclei at configuration. It means that a fusion reaction starting from 'compact' touching point results in a higher fusion probability than the fusion starting from a distant touching point. Consequently, the fusion process is greatly influenced by the relative orientations of the deformed nuclei. For heavy –ion fusion the 'gentle' fusion and "hugging fusion" have been proposed theoretically which correspond to some typical shapes of deformed nuclei(prolate deformed with positive or negative signs of hexadecapole deformations) and their relative orientations, it is relevant to mention here that the nuclear structure and orientations of the approaching heavy ions seem to affect minutely the mutual long range coulomb interaction ,as well as the short range nuclear potential.

Compact shapes are favorable in comparison to elongated shapes and an extra effort in form of "extra push energy" is required to form a stable nuclear system using elongated shapes.

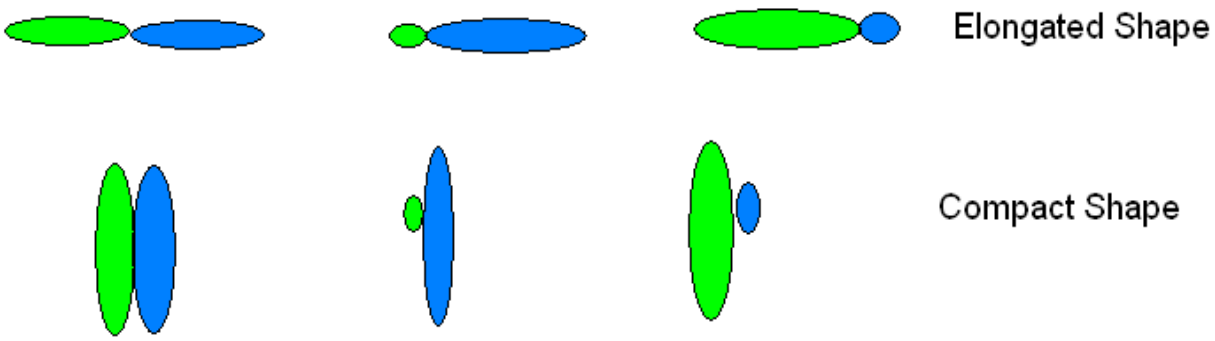


Figure.1.5. elongated & compact nuclear shapes of deformed interacting nuclear systems.

The inclusion of deformation and orientation effects of the colliding nuclei leads to lowering of its barrier height [3 -7].This means that the interaction potential and hence the fusion cross-sections are largely influenced by the nuclear structure effects of the target and projectile nuclei and their relative orientations . The collisions between deformed as well as oriented nuclei and their relative orientations. The collisions between deformed as well as oriented nuclei have been studied experimentally and theoretically to establish the effects of deformation and orientation on fusion reactions [3]-[7],[8]-[11]. According to these studies when deformed and oriented nuclei collide, the fusion barrier height varies leading to the barrier height distribution around the spherical coulomb barrier [5]. This distribution of the barrier height results in a substantial enhancement of fusion cross-sections in the region below spherical coulomb barrier.

A detailed study [5] based upon quantum mechanical fragmentation theory(QMFT) by gupta and collaborators shows that the interaction barrier (height as well as its position) is greatly affected by deformed and oriented colliding nuclei . The optimum orientations are given for “cold, non compact “ configurations leading to largest interaction radius and lowest barrier and “hot, compact” fusion configurations corresponding to smallest interaction radius and highest barrier, the details can be seen in table 1 of [5].

In heavy systems, the heavy ion fusion probability depends on the charge product $Z_1Z_2$ of projectile and target nuclei. When this charge product approaches ~1800 the probability of fusion shows a rapid decrease with increase in $Z_1Z_2$ [8] due to large coulomb repulsion. It is interesting to note that in the reaction of a heavy target-projectile combination, leading to heavier compound system , the crossing of a fusion barrier does not guarantee the formation of a CN. However, the system must overcome the saddle point of compound nucleus, which is located inside the fusion barrier between the heavy target and projectile. This hindrance in the fusion process is named as “extra-push” phenomenon and causes significant loss in the kinetic energy. But it has been observed that the favorable compact shape results more easily into CN rather than an elongated touching shape. Here, the favorable compact shape means that the distance between the mass centers of the nascent fission fragments at the fission saddle point. Hence, the relative distance between the mass centers of two colliding nuclei, with respect to saddle point, affects the fusion of heavy ions considerably.

For a system with large $Z_1Z_2$ product the contact point usually exists outside the saddle point. But in the fusion of deformed and relatively oriented nuclei the scenario is changed as at touching the distance between mass centres of massive reactants rely on the orientation of the deformed nuclei. It means that the fusion reaction starting from compact touching point results in higher fusion probability than the fusion starting from distant touching point. Thus the fusion process is greatly affected by the relative orientations of the deformed nuclei. In the fusion reactions involving deformed nuclei the quasi-fission and fusion –fission are in competition [9]. In the quasi-fission processes, incoming nuclei in a reaction do not loose its identity during the formation of CN and as a result such a non- equilibrated CN decays into fragments which are nearly the same as in the entrance channel i.e. projectile and target like fragments. Several

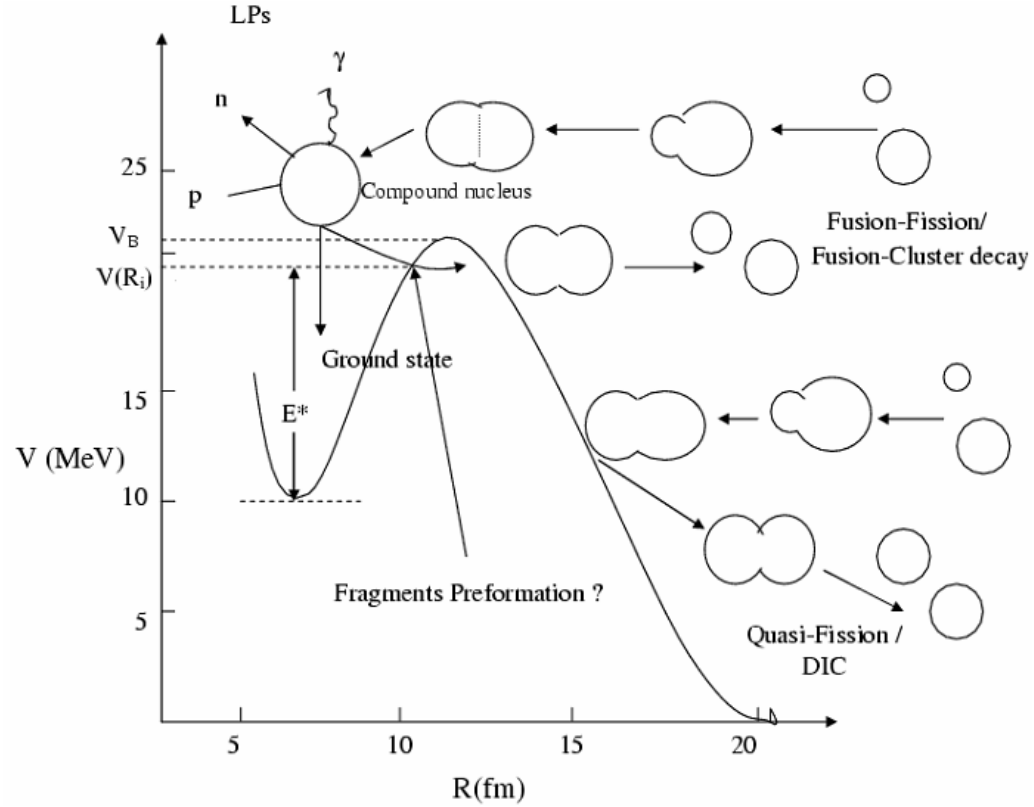


Figure1.6: schematic diagram for dynamics of the colliding nuclei playing around coulomb as well as nuclear interaction potential.

experimental studies show that the collision with tip to tip of deformed projectile-target nuclei lead to quasi-fission and the side collisions results in fusion fission [8],[9]. The terms like gentle fusion and hugging fusion have been coined theoretically[4], which correspond to typical shapes(prolate,oblate and higher multipoles) of deformed nuclei along with their relative orientations. It is relevant to mention here that the nuclear structure and orientations of the approaching heavy ions seem to affect the mutual long range coulomb interaction [12],[13] as well as the short range nuclear potential [3],[14].

Heavy ion fusion is not only affected by deformation and orientations of the reactants but also takes into account the nuclear shell structure of projectile and target nuclei . The shell closure of colliding nuclei plays a significant role in the sub-barrier fusion process[11],[15]. It indicates no fusion hindrance for the colliding nuclei with

nuclear shell closure structure. The target and projectile with this type of structure makes a compact touching shape and produces an equilibrated compound nucleus.

The nuclear reactions can also be categorized on the basis of energy of projectiles , as low, intermediate and high energy reactions. Projectiles with energies ≤10 MeV /nucleon and ≥ 400 MeV /nucleon cause low and high energy nuclear reactions respectively. Whereas the in between energy range corresponds to the intermediate energy reactions. In low energy reactions average/mean nuclear force field acting between the two nuclei dominate in comparison to high energy reactions where direct nucleon - nucleon interactions takes place. In intermediate energy reactions both the aspects play their role.

## 1.6 Super-heavy elements and Importance of Higher pole deformations

Now, the major challenge to experimental investigations is the increasing difficulty with which further heavier Super heavy Elements (SHEs) can be produced. The experimental work of last two decades has shown that in the synthesis of heavy nuclei with Z≥105, both in cold and hot fusion studies, the evaporation residue cross section $\sigma_{ER}$, taken as fusion cross-section, decreases rapidly with increasing Z of compound nucleus. In fact, at higher and higher atomic numbers the fusion reaction is a self-terminating process because of constantly increasing disruptive coulomb forces. Physics at this limit of cross-sections is difficult and challenging. Both the cold and hot fusion approaches have this common limitation in the available choice of target and beams. The available experimental methods for the synthesis of SHEs by cold fusion using(at least) one spherical closed shell target projectile nucleus, like Pb or Bi , have reached a limit of measuring capability i.e. 1pb for Z=112. However, very recently at RIKEN [16], the Z=113 element produced in $^{70}$Zi+$^{209}$Bi, reaction with cross-section of 55 fb is the smallest measured cross-section till to-date.

So far the above mentioned reactions have limited the experimentalist to the production of relatively neutron deficient isotopes of SHEs. But the real 'super-heavy Nucleus', referring to the centre of 'Island of Stability', with Z=114,120 or 126 and N=172 or 184, is still to be produced. Since there are number of questions to be answered still; like what are the borders of the super-heavy region and what are the properties of the heaviest nuclei that can be found(at least, theoretically) in spite of the huge disruptive coulomb force contribution.

One solution of this problem is the upgradation of machines used for the synthesis and detection of SHEs, which is quite expensive and tedious task. The other is to use neutron rich radioactive Nuclear beams(RNB) and radioactive nuclear targets (RNT) for the fusion reactions. In future, reactions between RNB and RNT may provide the best hope of mapping the entire region of shell stabilized nuclei around Z=114, 120 or 126 and N=172 or 184. However the required beam intensities will need to match and exceed those available for stable beam today if such experiments are to succeed. Thus, these studies may only become feasible with the next generation of radioactive beam facilities. Alternatively, we have to look for some other ways. This demands an extensive theoretical effort on the production cross-section of SHEs to explore a possible way for experimental designs. As a solution to this problem, many theoretical studies emphasize the use of deformed nuclei as both target and projectiles. Deformed nuclei can then be oriented either in the same plane (coplanar) or in different planes(non coplanar).

Collisions between deformed, oriented nuclei have been of much interest during last two decades. This concept may give the fusion of nuclei most probable at low energies and hence correspondingly fusion cross section can be increased. In early 1980's , this study got triggered off, beginning with a suggestion from Greiner[17] that oriented $^{238}U+^{238}U$ collisions could lead to a very long lived (life time~10-20sec) giant molecule. A number of calculations were made[18]-[22], all showing that the barrier is lowered due to deformations and orientations of colliding nuclei and that it is lowest for the $0^0$,$180^0$ orientations of two $^{238}U$ nuclei known as the pole to pole or nose to nose

configuration. Note that $^{238}U$ is a prolate deformed nucleus and hence the result is true only for prolate – prolate(p-p) collisions. For fusion studies , the position of barrier is also important [23], and then the role of quadrupole and higher multipole deformations comes, which has also become important recently[24]-[31].

The role of higher multipole deformations is also studied for cold fusion reactions , very recently by Misicu and Greiner[27], but for arbitrary ori entations only. The "optimum" orientations [30] for both the hot and cold fusion reactions, for a given pair of deformed nuclei using the proximity potential based on Blocki et al.[32,33]. This study shows that "the choice of orientations of reaction parteners for cold and hot fusion depend on the signs of quadrupole deformations and are independent of signs of hexadecupole deformations". However, later study of Gupta, et.al. [29] showed that the choice of optimum orientations, i.e., the most compact orientations for hot fusion and the most elongated orientations for cold fusion depends on the magnitudes of both the quadrupole and hexadecupole deformations of the deformed reaction parteners.

They observed that the pure quadrupole deformed nuclei and the nuclei with normal (large or small) quadrupole deformation plus small-positive or negative hexadecupole deformations result in an equatorial configuration(ec,$\Theta=90^0$), and the ones with normal (large or small) quadrupole deformation plus large-positive hexadecupole deformation gives rise to a not-equatorial configuration (nec, $\Theta < 90^0$). Interestingly, they have shown that all compound systems with $Z \geq 114$ nuclei are compact at the orientation angle $\Theta=90^0$ (collisions in the direction of minor axis of the deformed nucleus),the so called "equatorial compact"(ec) configuration and that the same for $Z<114$ are compact at $70^0$, referred to as "not equatorial compact"(nec) configuration .

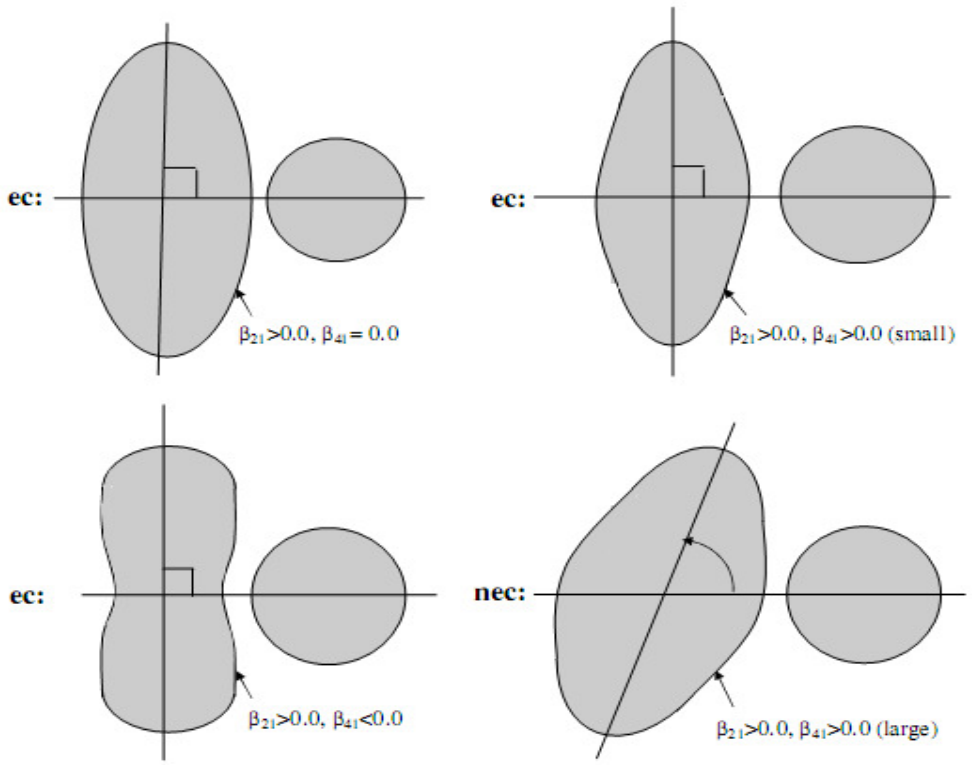


Figure1.7

Representative ec/nec hot fusion configurations of (prolate) deformed+ spherical nuclei, for different magnitudes of hexadecupole deformations. The ec and nec refer, respectively, to the orientation of deformed nucleus at $\Theta=90^0$ and $\Theta<90^0$.

Fig1.7. shows some of the compact hot fusion configurations, which are discussed with respect to the different magnitudes of $\beta_4$. It has been found in Fig1.7. that the compact angle of orientation being approximately $70^0$ for "nec" as compared to $90^0$ for "ec". [29]. So the "nec" configuration is considerably different from "ec";

Experimentally, the role of deformation and orientation degrees of freedom in the measurement of capture cross sections have been pointed out in some very recent experiments [34,35] for $^{238}U+^{48}Ca$, $^{242,244}Pu+^{48}Ca$ and $^{248}Cm+^{48}Ca$ using hot fusion reactions. The increased fusion threshold is associated with the static deformations of the target nuclei, whose orientations at the point of collision leads to various configurations of the composite system at the very start of its path toward the spherical shape of the compound nucleus. Thus, the configurations based on deformed and

oriented nuclei will be very decisive for determining the fusion and capture cross sections. Therefore , one can expect that the use of deformed and oriented nuclei would promote a better understanding of the stability of superheavy elements and represents the processes that lead to the fusion of heavier nuclei. The explicit role of deformations and orientations certainly improve our understanding regarding the dynamics of a nuclear system.

## 1.7 References:


[1] ^ Irvine, J. M. 1972, 'Nuclear Structure Theory', Pergamon Press, Oxford

[2]. Casten , R. 1990, 'Nuclear structure from a simple perspective ' Oxford University Press, New York.

[3]. N. Malhotra and R.K.Gupta, Phys. Rev. C 31,1179 (1985).

[4]. A. Iwamoto, P. Moller, J.R. Nix, and H. Sogawa, Nucl. Phys. A596, 329-354 (1996).

[5]. R.K.Gupta, M. Balasubramaniam, R. Kumar, N.Singh, M.Manhas, and W. Greiner, J. Phys. G: Nucl. Part. Phys. C 31, 631 (2005).

[6]. M. Manhas and R.K.Gupta, Phys. Rev. C 72, 024606 (2005).

[7]. R.K.Gupta, M. Manhas, G. Munzenberg and W. Greiner, Phys. Rev. C 72, 014607 (2005).

[8]. K. Nishio, H. Ikezoe, S. Mitusuoka and K. Satou and S.C. Jeong, Phys. Rev. C 63, 044610 (2001).

[9]. D.J. Hinde, M. Dasgupta, J.R. Leigh, J.P. Lestone, J.C. Mein, C.R. Morton, J.O. Newtn, and H.Timmers, Phys.Rev. Lett. 74, 1295 (1995).

[10]. M. Dasgupta, D.J. Hinde, J.R. Leigh and K. Hagino, Nucl. Phys. A630, 78C (1998).

[11]. Yu. Ts. Oganessian; Heavy Elements and Related New Phenomena, edited by W. Greiner and R.K.Gupta, World Scientific, Singapore, P. 43, (1999).

[12]. C.Y. Wong, Phys. Lett. 26B,120 (1968).

[13]. L. Wilets, E. Guth, and J.S. Tenn, Phys. Rev. 156, 1349 (1967); H.Holm, W Scheid, and W. Greiner, Phys. Lett. 24, 404 (1970); A.S. Jensen and C.W. Wong, Phys. Rev. C 1,1321 (1970); P.W. Riesenfeldt and T.D. Thomas, ibid. 2, 711 (1970).

[14]. M. Seiwert, W.Greiner, V. Oberacker, and M.J. Rhoades-Brown, Phys. Rev. C 29, 477(1984).

[15]. H. Ikezoe, S.Mitsuoka, K. Nishio, K.Satou, and I.Nishinaka, J.Nucl. and Radiochemical Sciences, 3, 39 (2002).

[16]. K. Morita, et al., J. Phys. Soc. Japan 73, 2593 (2004)

[17]. W. Greiner, International NATO Advanced study Institute (NASI) course on quantum Electrodynamics of strong Fields, Lahnstein 1981;

M. Seiwert, N. Abul-Naga , V. Oberacker, J.A. Maruhn and W. Greiner, Gesellschaft fur Schwerionenforschung(GSI) Annual Report 1981.

[18]. A.J. Baltz and B.F.Bayman, Phys.Rev.C 26,1969 (1982).

[19]. M. Munchow , D. Hahn and W.Scheid , Nucl. Phys. A 388, 381 (1982).

[20]. M.J. Rhoades-Brown, V.E. Oberacker , M.Seiwert and W.Greiner, Z.Phys. A 310, 287 (1983).

[21]. M.Seiwert, W. Griener , V. Oberacker , M.J. Rhoades-Brown, Phys. Rev. C 29, 477 (1984).

[22]. N. Malhotra and R.K. Gupta, Phys.Rev. C 31, 1179 (1985).

[23] . R.K. Gupta, A. Sandulescu and W. Grenier , Phys. Lett. 67B, 257 (1977); Rev. Roum . Phys.23, 51 (1978).

[24]. A. Iwamoto, P. Moller, J.R. Nix, and H. Sagawa, Nucl. Phys. A 596, 329 (1996).

[25]. W. Norenberg, GSI Nachrichten 10-94 (1994), p.13;

Proceedings of International Workshop on Heavy Ion Fusion, Padava, Italy (World Scientific Publications , Singapore 1994), p.248.

[26]. S. Misicu and W. Greiner, Phys. Rev. C 69, 054601 (2004).

[27]. S. Misicu and W. Greiner, Phys. Rev. C 66, 044606 (2002).

[28]. M. Manhas and R.K. Gupta, Phys. Rev. C 72, 024606 (2005).

[29]. R.K. Gupta, M. Manhas, and W. Greiner, Phys. Rev. C 73, 054307 (2006).

[30]. R.K. Gupta, M. Balasubramaniam, R. Kumar , Narinder Singh , M. Manhas, and W. Greiner, J. Phys. G: nucl. Part. Phys. 31, 631 (2005).

[31]. R.K. Gupta, M. Manhas, G. Munzenberg , and W. Greiner, Phys. Rev. C 72, 014607(2005).

[32]. R.K. Gupta, Narinder Singh, and M. Manhas, Phys. Rev. C 70, 034608 (2004).

[33]. J. Blocki, J. Randrup, W.J. Swiatecki, and C.F. Tsang , Ann. Phys. (NY) 105, 427 (1977).

[34]. Yu.Ts. Oganessian et al ., Phys.Rev . C 69, 054607 (2004)

[35]. Yu.Ts. Oganessian , et al ., Phys. Rev. C 70, 064609 (2004).

# Chapter 2
# METHODOLOGY

## 2.1 INTRODUCTION

A comprehensive study of various types of emission from the ground state as well as excited states of compound nucleus (CN) formed in low energy reaction is important, as it gives information about the nuclear structure aside the underlying nuclear forces .At low energies and average nuclear force field acts between decaying fragments which in turns ensure possibility of more than one decay path .This average nuclear force field is largely influenced by entrance channel, angular momentum and the temperature consideration along with contribution of deformed and orientation effects. An extensive study of these nuclear properties lead to a better understanding of reaction dynamics of rare nuclear species that make the unexplored part of the nuclear chart, called exotic nuclei.

The main aim of the work is to study heavy ion reaction dynamics especially the decay of excited compound nucleus using the dynamical cluster decay model(DCM)[1]-[9].It is important to note that deformation and orientation effects of the reaction partner and decay products are explicitly included along with temperature and angular momentum contribution in this model. The ground state cluster decay of radioactive nuclei have also been undertaken with in the preformed cluster decay model [10]-[18].Again having deformation and orientation effects of the cluster as well as daughter nuclei included in it. Details of DCM and PCM are given in the section 2.2 and 2.6 respectively both of which stem from the Quantum Mechanical Fragmentation

Theory, (QMFT)[19]-[32] which in binary fragmentation, uses a collective mass transfer process.

This model is a two step model ,where the first step is quantum mechanical preformation probability $P_0$ of the decay products or cluster formed in the mother nuclei and the second step is the penetration of the fragments/ clusters through the interaction barrier. The $P_0$ based on QMFT is also discussed here in section 2.3.7. The details for penetration probability P are given in section 2.4. These two crucial parameters ($P_0$and P) have been developed and used[9],[17],[18],[33,][34], to incorporate the deformation effects of oriented nuclei. The assault frequency, $\nu_0$ with which the preformed cluster tries to tunnel the barrier in the ground state decay is discussed in section 2.5

## 2.2 THE DYNAMICAL CLUSTER DECAY MODEL (DCM) FOR HOT AND ROTATING COMPOUND NUCLEUS

The dynamical cluster decay model (DCM) [1]-[9] for hot and rotating nuclei (i.e. angular momentum and temperature both not equal to zero) is a reformation of the preformed cluster model of Gupta and collaborators for ground state decay ($\ell$ =0,t=0)in cluster radioactive (CR)and related phenomena [10]-[18] .like PCM and DCM is also based upon the dynamical (or quantum mechanical) fragmentation theory of cold phenomena in heavy ion reaction and fission dynamics .In DCM, besides the temperature and angular momentum effects in the decay of excited compound nuclei ,the deformation and orientation effect of the decay products are also taken care, especially in the decay of heavy excited CN for which the deformation of the decay product seems to play significant role. The DCM, worked out in terms of the collective coordinates of mass asymmetry $\eta=\frac{A_1-A_2}{A_1+A_2}$ and relative separation R respectively gives

(i). The nucleon-division (or exchange )between the outgoing fragments ,and

(ii). The transfer of kinetic energy of incident channel ($E_{cm}$) to internal excitation (total excitation or total kinetic energy ,TXE or TKE) of the outgoing channel .It may be noted that the fixed decay point R = $R_a$ (defined later),at which the process is calculated depends upon temperature T as well as on $\eta$ (i.e.R(T,

η)) .This energy transfer process can be calculated as follows with the help of Fig 2.1

$\mathbf{E}^{*}_{\mathbf{CN}}$ = $E_{c.m} + Q_{in} = |Q_{out}| + TKE(T) + TXE(T)$

The CN excitation $\mathbf{E}^{*}_{\mathbf{CN}}$ is related to T (in Mev ) and is given by

$\mathbf{E}^{*}_{\mathbf{CN}} = \frac{1}{9}AT^2 - T(Mev)$ . Using the decoupled approximation to R and η–motions, the DCM define the decay cross section ,in terms of partial waves,as[3]-[9] ;

$$k=\sqrt{\frac{(2\mu E_{c.m})}{\hbar^2}}; \sigma = \sum_{l=0}^{lc} \sigma l = \frac{\pi}{k^2}\sum_{l=0}^{lc}(2l+1)P_oP \qquad (2.2)$$

Where $P_o$ ,the preformation probability refers to η-motion and P, the penetrability to the R- motion, discussed in section 2.3.7 and 2.4 respectively .Here the complex fragments (both light and heavy fragments) are treated as the dynamical collective mass motion of preformed cluster or fragments through the barrier .The structure information of the CN enters the model vai preformation probability $P_o$ (also known as spectroscopic factor )of the fragments given by the solution of stationary Schrödinger equation in η at the fixed $R=R_a$ ,the first turning point of the penetrability path shown in figure 2.1for the different l-values .

$$\left\{-\frac{\hbar^2}{2\sqrt{B_{\eta\eta}}}\frac{\partial}{\partial\eta}\frac{1}{\sqrt{B_{\eta\eta}}}\frac{\partial}{\partial\eta}+V_R(\eta,T)\right\}\psi^{\nu}(\eta)=E^{\nu}\psi^{\nu}(\eta) \qquad (2.3)$$

with $\nu$ =0,1,2,3,….referring to the ground state and excited state solution .

For the decay of the hot compound nucleus, we use the postulate of first turning point

$$R_a=R_t+\Delta R(T) \qquad (2.4)$$

Where

$$R_t = R_1+R_2 \qquad (2.5)$$

ΔR(T) is the neck length parameter that assimilates the neck formation effects .This method is introducing a neck length parameter similar to that used in scission point [35] and saddle point [36],[37]statistical fission model.The $R_i$ are radius vectors which are also made temperature dependent can be calculated as

$$R_i(\alpha_i) = R_{0i}\left[1 + \sum_{\lambda} \beta_{\lambda i} Y_{\lambda}^{(0)}(\alpha_i)\right] \tag{2.6}$$

with

$$R_{0i}(T) = 1.28A_i^{1/3} - 0.76 + 0.8A_i^{-1/3} \times (1 + 0.0007T^2), \tag{2.7}$$

The corresponding potential V ($R_a$) acts like an effective Q-value, $Q_{eff}$ , for the decay of the hot CN at temperature T, to two exit-channel fragments observed in g.s. (T=0), defined by

$$Q_{eff}(T) = B(T) - [B_L(T = 0) + B_H(T = 0)]$$
$$= TKE(T) = V(R_a(T)) \tag{2.8}$$

with B's as the respective binding energies.

The above defined decay of a hot CN into two cold (T=0) fragments, via Eq.(2.8), could apparently be achieved only by emitting some light particle (s)(LPs), like n, p, α, or γ-rays of energy

By defining $Q_{eff}$ (T) as in Eq. (2.8), in this model we treat the LP emission at par with the heavy fragments, called intermediate mass fragments (IMFs) emission. Thus, in this model a non-statistical dynamical treatment is attempted for not only the emission of IMFs but also of multiple LPs, understood so-far only as the statistically evaporated particles in a CN emission. It may be reminded here that the statistical model (CN emission) interpretation of IMFs is not as good as it is for the LP production [35–40].

In terms of $Q_{eff}$ (T), the second turning $R_b$ satisfies (see Fig. 2.1)

$$V(R_a, l) = V(R_b, l) = Q_{eff}(T, l) = TKE(T). \tag{2.9}$$

with the l-dependence of $R_a$ defined by

$$V(R_a, l) = Q_{eff}(T, l = 0), \tag{2.10}$$

which means that the $R_a$, given by Eq. (2.4), is the same for all $l$ -values, and that V (Ra, $l$) acts like an effective Q-value, $Q_{eff}$ (T, $l$), given by the total kinetic energy TKE(T). Then, using (2.9), $R_b(l)$ is given by the $l$ -dependent scattering potentials, at fixed Tas

$$V(R, T, l) = V_c(Z_i, \beta_{\lambda i}, \theta_i, T) + V_p(A_i, \beta_{\lambda i}, \theta_i, T)$$

$$+ V_{\ell}(R, A_i, \beta_{\lambda i}, \theta_i, T) \qquad (2.11)$$

which is normalized to the exit channel binding energy $B_L(T) + B_H(T)$. Such a potential is illustrated in Fig. 2.1, $^{132}Sn+^{64}Ni \rightarrow ^{196}Pt$, at different $\ell$ -values. The second turning point $R_b$ is marked for the $\ell = 0\hbar$ case of $R_a = R_t + \Delta R(T)$.Note that as the $\ell$ -value increases, the $Q_{eff}$ (T)-value ( =TKE(T)) increases and hence V ($R_a$, $\ell$ ) increases, since the decay path for all the $\ell$ -values begins at R = $R_a$.

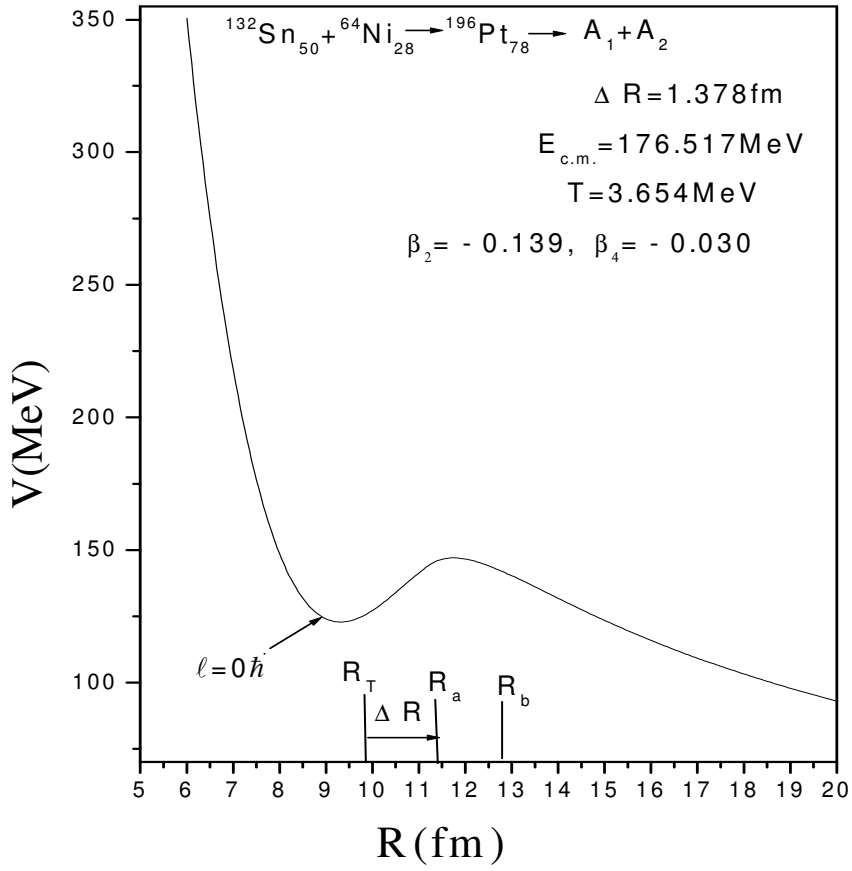


Fig.2.1. Scattering Plot for $^{132}Sn+^{64}Ni \rightarrow ^{196}Pt$ reaction

The collective fragmentation potential V (R, η, T) in Eq. (2.11) is calculated according to the Strutinsky method by using the T-dependent liquid drop model energy $V_{LDM}$ of [41], with its constants at T=0 re-fitted [3, 4] to give the recent experimental binding energies given by [42], and again refitted [9] to give the recent experimental binding energies[43] and calculate binding energies[44] (only for those

nuclides for which experimental data is not available. the “empirical” shell corrections δU are of Ref. [45] (In the Appendix of [3] and Eq. (8) of [4], $a_a$=0.5, instead of unity). Then, including the T-dependence also in Coulomb, nuclear proximity, and $l$ -dependent potential in complete sticking limit of moment of interia , we get

$$V(R,\eta,T) = \sum_{i=1}^{2}[V_{LDM}(A_i,Z_i,T) + \sum_{i=1}^{2}[\delta Ui]\,exp\left(\frac{-T^2}{T_0^2}\right) + V_c(Z_i,\beta_{\lambda i},\theta_i,T) + V_p(A_i,\beta_{\lambda i},\theta_i,T) + V_l(R,\beta_{\lambda i},\theta_i,T) \quad (2.12)$$

where the T-dependent terms $V_c$, $V_P$ and $V_i$ are defined as follows: The proximity potential for hot deformed nuclei is [33],[34] (see section 2.3.3)

$$V_p(A_i, \beta_{\lambda i}, \theta i, T) = 4\pi\bar{R}\,(T)\gamma b(T)\Phi(s_0(T)) \quad (2.13)$$

and, the Coulomb Potential (see section 2.3.4)

$$V_c\left(Z_i,\beta_{\lambda i},\theta_i,T\right) = \frac{Z_1 Z_2 e^2}{R(T)} + 3Z_1Z_2e^2 \sum_{i,i=1,2}\frac{R_i^{\lambda}(\alpha_i,T)}{(2\lambda+1)R(T)^{\lambda+1}} Y_\lambda^{(0)}(\theta_i)\left[\beta_{\lambda i} + \beta_{\lambda i}^2 Y_\lambda^{(0)}(\theta_i)\right] \quad (2.14)$$

with the radius vector given by Eq. (2.6) and surface thickness parameter

$$b(T) = 0.99(1 + 0.009T^2). \quad (2.15)$$

The angular momentum potential, (see section 2.3.5)

$$V_l\,(R,A_i, \beta_{\lambda i}, \theta_i, T) = \frac{\hbar^2\, l\,(l+1)}{2I_s(T)} \quad (2.16)$$

with the moment-of-inertia,

$$I_s(T) = \mu R^2 + \frac{2}{5}A_1 m R_1^2(\alpha_1, T) + \frac{2}{5}A_2 m R_2^2(\alpha_2, T).$$

Further, in Eq. (2.12), within the Strutinsky renormalization procedure, we have defined the binding energy B of a nucleus at temperature T as the sum of liquid drop energy $V_{LDM}(T)$ and shell correction δU(T) i.e

$$B(T) = V_{LDM}(T) + \delta U \exp\left(\frac{-T^2}{T_0^2}\right) \quad (2.17)$$

The T dependent liquid drop part of the binding energy VLDM(T) is from Davidson et al. [41], based on the semi-empirical mass formula of Seeger [46]. For the shell correction

δU in Eq. (2.17), since there is no microscopic shell model known that gives the shell corrections for light nuclei, we use the empirical formula of Myers and Swiatecki [45].

The mass parameters $B_{\eta\eta}(\eta)$, representing the kinetic energy part in Eq. (2.3),are the smooth classical hydrodynamical masses [47], given by Eq. (2.60) (in the section 2.3.6) for $\upsilon_1 = \upsilon_2 = 0^0$ and $R_i$ taken as temperature dependent.

Finally, the $l_c$-value in Eq. (2.6) is the critical l-value, in terms of the bombarding energy $E_{c.m.}$, the reduced mass μ and the first turning point $R_a$ of the entrance channel $\eta_{in}$, given by

$$l_c = R_a\sqrt{(2\mu[E_{c.m.} - V(R_a, \eta_{in}, l = 0)])}/\hbar \qquad (2.18)$$

or, alternatively, it could be fixed for the vanishing of fusion barrier of the incoming channel, called $l_{fus}$, or else the $l$-value ($l_{max}$) where the light-particle cross section $\sigma_{LP} \rightarrow 0$. This, however, could also be taken as a variable parameter [36,48].

## 2.3 QANTUM MECHANICAL FRAGMENTATION THEORY

In QMFT [19]-[32], the essential quantities for the description of the nuclear dynamics are the potential energy surfaces and the mass parameters defining the kinetic energy of the system while the static properties of nuclear system are determined by the potential energy only. The QMFT is worked out in terms of the following collective variables:

(1) relative separation coordinate R between the two nuclei or, in general two fragments (or, equivalently, the length parameter $\lambda = L/2R_0$, with L as the length of the nucleus and $R_0$ as the radius of an equivalent spherical nucleus).

(2) The deformation co-ordinates $\beta_{\lambda i}$ ($\lambda$=2,3,4…. and i=1,2) of the colliding nuclei.

(3) The orientation degrees of freedom $\Theta_i$ ( i= 1,2) of the deformed nuclei(fig. 2.2)

(4) Azimuthal angle Φ between the principles planes of the two colliding nuclei.

(5) Neck parameter ε, defined by the ratio $\varepsilon = E_0/E'$ for the interaction region ($R < R_1+R_2$, $R_i$ (i=1,2) is the radius of the two nuclei);

Where $E_0$ is the actual height of the barrier and E' is the fixed barrier of the two centre oscillator. ε = 0 represents a broad neck formation, whereas ε= 1 gives that the neck is fully squeezed in, corresponding to the asymptotic region ($R > R_1+R_2$).

(6) Mass and charge fragmentation co-ordinates[19],[20],[31].

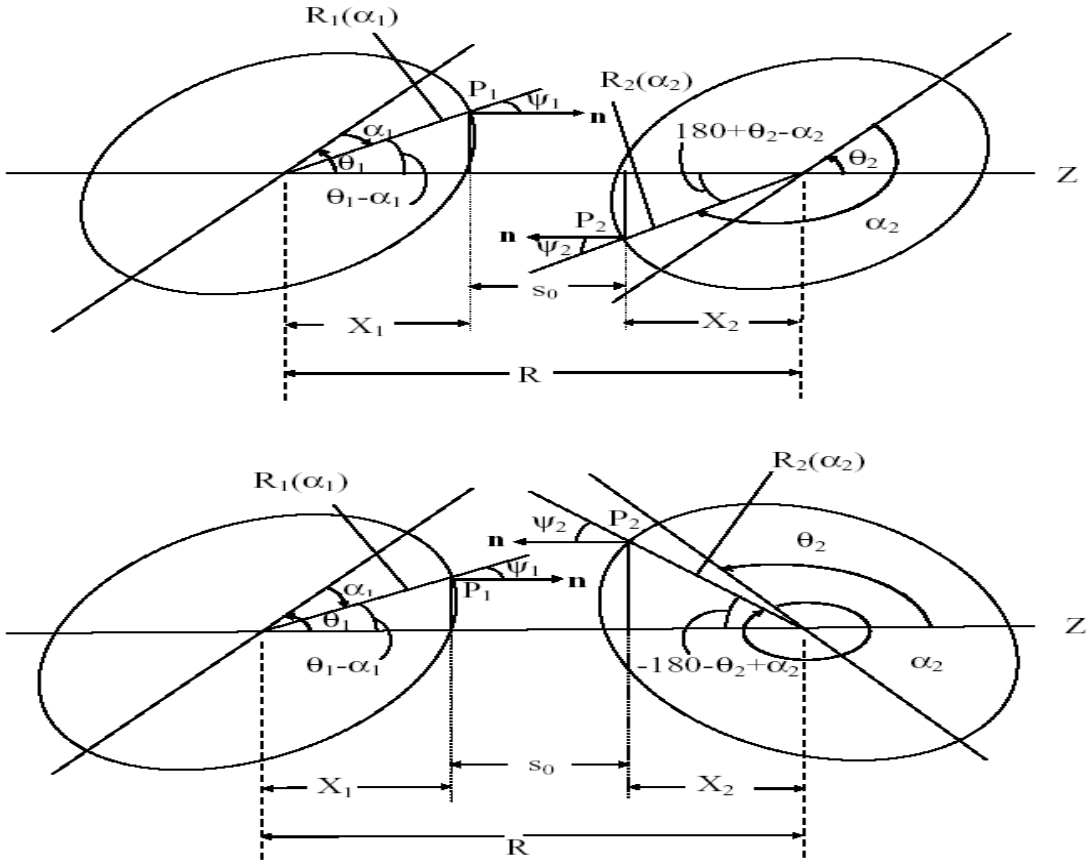


Figure 2.2: Schematic configurations of two (equal/ unequal) axially symmetric deformed, oriented nuclei, lying in the same plane and for various $\Theta_1$ and $\Theta_2$ values in the range $0^0$ to $180^0$. The $\Theta$'s are measured in anti-clockwise from the colliding axis and the angle $\alpha$'s in clockwise from the symmetry axis.

For two body channels, the mass and charge fragmentations for separated nuclei/fragments are defined by the mass and charge-asymmetry coordinates as

$$\eta = \frac{A_1 - A_2}{A}; \qquad \eta_Z = \frac{Z_1 - Z_2}{Z} \tag{2.19}$$

similarly, the neutron asymmetry coordinate [20]

$$\eta_N = \frac{N_1 - N_2}{N} \tag{2.20}$$

can also be used, but it is sufficient to treat only two of them as dynamical co-ordinates since they are related as

$$\eta = \frac{Z}{A}\eta_Z + \frac{N}{A}\eta_N \qquad (2.21)$$

Here $A=A_1+A_2$, $Z=Z_1+Z_2$ and $N=N_1+N_2$. $A_i$, $Z_i$ and $N_i$ (i = 1, 2) are respectively the mass number, the charge number and the neutron number of two fragments. A, Z and N are respectively the mass number, charge number and neutron number of the compound nucleus system. The limiting values of η are $0 \leq |\eta| \leq 1$ and thus allows a unified description of a few – nucleon or multi - nucleon (a cluster) transfer , a large-mass transfer, the complete fusion ($|\eta| = 1$) of nuclei and the symmetric ($\eta = 0$), asymmetric and super-asymmetric fission of a nucleus or compound nucleus. The $\eta_Z$ coordinate gives the associated charge distribution effects. In terms of these collective coordinates and their velocities, the collective Hamiltonian can be written as( taking β to stand for $\beta_{\lambda 1}$ and $\beta_{\lambda 2}$ ($\lambda$=2,3,4….))

$$H = K(\varepsilon, \beta, \eta_z, R, \eta, \dot{\eta_z}, \dot{R}, \dot{\beta}, \dot{\eta}, \dot{\varepsilon}) + V(\varepsilon, \beta, \eta_z, R, \eta) \qquad (2.22)$$

For the compound nucleus formation, the neck parameter ε=0 is assumed, since once the neck formation starts between the two colliding nuclei, then fission phenomenon takes place, i.e. excited compound nucleus will proceed towards the disintegration process.

For the potential $V(\eta, \eta_Z, R)$, minimized in the $\eta_Z$ coordinate, Schrödinger wave equation in terms of mass parameters η and relative separation R co-ordinate can be written as:

$$H(\eta, R)\Psi(\eta, R) = E(\eta, R)\,\Psi(\eta, R) \qquad (2.23)$$

With the Hamiltonian,

$$H(\eta, R) = K(\eta) + K(R) + K(\eta, R) + V(\eta) + V(R) + V(\eta, R) \qquad (2.24)$$

Here, K refers to the kinetic energy and V to the collective potential energy. The mass parameters $B_{ij}$. Defining the kinetic energy term K in the above Eqs.(2.24) and (2.26) are either the consistently calculated cranking masses using the Asymmetric shell model

(ATCSM) or the classical hydrodynamical masses, which are shown to have good agreement with microscopic cranking calculations.

The coupling term of the kinetic energy K (η,R), proportional to $\partial^2/(\partial_\eta \partial_R)$, is neglected here, since the coupled cranking masses are very small [19],[20] ($B_{R\eta} << (B_{RR}B_{\eta\eta})^{1/2}$ and $B_{R\eta Z} << (B_{RR}B_{\eta Z\eta Z})^{1/2}$). Same is true for the coupling term of potential energy V (η,R). Therefore, in a decoupled approximation [32] , the schrodinger equation (2.25) can be solved for which the hamiltonain takes the form:

$$H = \frac{-\hbar^2}{2\sqrt{B_{\eta\eta}}}\frac{\partial}{\partial_\eta}\frac{1}{\sqrt{B_{\eta\eta}}}\frac{\partial}{\partial_\eta} - \frac{\hbar^2}{2\sqrt{B_{RR}}}\frac{\partial}{\partial_R}\frac{1}{\sqrt{B_{RR}}}\frac{\partial}{\partial_R} + V(\eta) + V(R) \qquad (2.25)$$

For decoupled Hamiltonian (2.7), schrodinger wave equation (2.23) can be separated for the two co-ordinates η and R as follows,

$$\left[\frac{-\hbar^2}{2\sqrt{B_{\eta\eta}}}\frac{\partial}{\partial_\eta}\frac{1}{\sqrt{B_{\eta\eta}}}\frac{\partial}{\partial_\eta} + V(\eta)\right]\Psi^v(\eta) = E_\eta^v \Psi^v(\eta) \qquad (2.26)$$

$$\left[\frac{-\hbar^2}{2\sqrt{B_{RR}}}\frac{\partial}{\partial_R}\frac{1}{\sqrt{B_{RR}}}\frac{\partial}{\partial_R} + V(R)\right]\Psi^v(R) = E_R^v \Psi^v(R) \qquad (2.27)$$

With $\psi(\eta,R) = \psi(\eta)\psi(R)$ (2.28)

$$E = E_\eta + E_R \qquad (2.29)$$

The states $\Psi^v(\eta)$ are the vibrational states in the potential V(η) and are labeled by the quantum numbers $v$ =0,1,2……

In the following subsections, we first discuss the various the various terms of schrodinger wave equations (2.26) and (2.27) and then give the solution of Eq. (2.26) for the determination of preformation probability $P_0 \propto |\psi^0(\eta)|^2$.

.

## 2.3.1The Scattering Potential V(R)

For a fixed η i.e. for a given outgoing fragment ($A_1$,$A_2$) combination, the scattering potential V(R) in Eq. (2.27) is defined as the sum of the deformations, orientations dependent coulomb potential, proximity potential and angular momentum dependent potential, i.e.

$$V(R) = V_c(R, Z_i, \beta_{\lambda i}, \theta_i, \Phi) + V_p(R, A_i, \beta_{\lambda i}, \theta_i, \Phi) + V_\ell(R, A_i, \beta_{\lambda i}, \theta_i, \Phi) \quad (2.30)$$

## 2.3.2 The Fragmentation potential V(η)

The collective potential energy or the fragmentation potential V(η,R), appearing in equation (2.8) is calculated as,

$$V(\eta,R) = \sum_{i=1}^{2} Bi(Ai, Zi\ \beta\lambda i) + Vc(R, Zi, \beta\lambda i, \theta i, \varphi) + Vp(R, Ai, \beta\lambda i, \theta i, \varphi) + V_\ell(R, Ai, \beta\lambda i, \theta i, \varphi) \quad (2.31)$$

Here $B_i$ (i=1,2) are the binding energies of the two nuclei, available from the experimental data of Audi-wapstra [43]. Wherever the experimental B's are not available, the theoretical binding energies of Moller et al.[44] are used. Note that the binding energies contain both the macroscopic (liquid drop part) and the microscopic (shell correction part).

The fragmentation potential V (η) is calculated at a fixed distance $R=R_1+R_2+\delta R$ or $R=C_1+C_2+\delta C$ fm, with $C_i$ (i=1,2) as the sussmann central radii related to the radius vector $R_i$ as $C_i = R_i(1 - b^2/R_i^2)$ with

$$R_i = R_{0i}\left[1+\sum_\lambda \beta\lambda i\, Y_\lambda^{(0)}(\alpha i)\right], \quad (2.32)$$

and

$$R_{0i} = 1.28A_i^{1/3} - 0.76 + 0.8A_i^{-1/3} \quad (2.33)$$

Here λ=2,3,4…. and $\alpha_i$ is an angle that the radius vector $R_i$ of the colliding nuclei makes with the symmetry axis(fig.2.2) the diffuseness of the nuclear surface (I.e. the surface thickness) b = 0.99 fm. The charges $Z_i$ are fixed by minimizing the potential V (η) in the $\eta_Z$ coordinate at each η value.

For the study of excited systems, where the nuclear temperature effects also come into picture, the fragmentation potential at fixed R is

$$V(\eta, T) = \sum_{i=1}^{2} V_{LDM}(A_i,Z_i, T) + \sum_{i=1}^{2} \delta U \exp(-T^2/T^2_0) + V_c(Z_i, \beta_{\lambda i}, \theta_i, \varphi, T) + V_p(A_i, \beta_{\lambda i}, \theta_i, \varphi, T) + V_\ell(A_i, \beta_{\lambda i}, \theta_i, \varphi, T) \quad (2.34)$$

Here, $V_{LDM}$ ($A_i$, Zi, T) is the liquid drop part of the binding energy and δU, the shell corrections. Note that the calculation of fragmentation potential involves all the possible decay channels and the number of all such possible decay channels becomes more and more with the increasing mass of the mother nucleus. The nuclear temperature T (in MeV ) is related to the excitation energy $E^*_{CN}$ of the compound nucleus, through a semi-empirical statistical relation as:

$$E^*_{CN} = 1/10AT^2 - T \ \text{(MeV)} \qquad (2.35)$$

The shell corrections δU in Eq. (2.34) are considered to vanish exponentially for $E^*_{CN} \geq 60$ MeV , giving $T_0 = 1.5$ MeV . At higher excitation energies the shell corrections vanish completely and only the liquid drop part of energy is present. The shell corrections play an important role in determining or empirical fitting of nuclear masses, because the nuclear masses calculated by using the smooth liquid drop formula show large deviations with respect to the experimental masses. It means that in the experimental masses there exist deep minima at specific neutron and/or proton numbers indicating the presence of shell structure, the so-called magic numbers in nuclei. This characteristic behavior cannot be reproduced by the liquid drop part alone, which means that the introduction of microscopic shell correction in the mass formula is essential. Thus, shell corrections accounts for the removal of deviation from the liquid drop calculations (uniform distribution of nucleons), and are defined, within Strutinsky [49] method as

$$\delta U = U - \tilde{U} \qquad (2.36)$$

where, $U = \sum_\nu E_\nu 2n_\nu$ is the sum over all occupied single particle states and

$$\tilde{U} = \int_{-\infty}^{\tilde{\jmath}} E\tilde{g}(E)dE \qquad (2.37)$$

is the average energy for uniform distribution. In general, the microscopic shell correction, together with the liquid drop part, gives a proper description of the binding

energy of the nucleus. This method, however, does not give a proper description of light mass nuclei. The difficulty is the inadequacy of shell model for very light nuclei. For this reason, the macro-microscopic calculations of Moller et al. [44] are tabulated for $Z \geq 8$ only. For $Z \leq 8$, one could alternatively use the empirical shell correction method of Myers-Swiatecki [38] which again is not very satisfactory for light nuclei ($Z \leq 16$). Gupta and collaborators have modified this empirical method and obtained a better description of the shell corrections for the light as well as heavy mass region, i.e, $1 \leq Z \leq 118$ [4].

### 2.3.3The Proximity Potential for deformed, oriented and coplanar nuclei

When two surfaces approach each other within a small distance of less than ~ 2fm, comparable with the surface thickness of interacting nuclei, or when a nucleus is at the verge of dividing into two fragments, then the two surfaces actually face each other across a small gap or crevice. In both cases, the surface energy term alone could not give rise to the strong attraction that is observed when the two surfaces are brought in close proximity. Such additional attractive forces are called proximity forces and the additional potential due to these forces is called the nuclear proximity potential.

Blocki et al. [50] have reanalyzed and extended a theorem, originally due to Deryagin [51], according to which the force between two gently curved surfaces in close proximity is proportional to the interaction potential per unit area between the two flat surfaces. The original expression of Blocki based on the pocket formula was for spherical nuclei, and is given as

$$V_P(s_0) = 4\pi\overline{R}\gamma b\Phi(s_0). \qquad (2.38)$$

$\Phi(s_0)$ is the universal function, independent of the shapes of nuclei or the geometry of nuclear system, but depends on the minimum separation distance

$$\Phi(s_0) = \begin{cases} -1/2(s_0 - 2.54)^2 - (s_0 - 2.54)^3 \\ -3.437\exp(-s_0/0.75) \end{cases} \qquad (2.39)$$

respectively, for $s_0 \leq 1.2511$ and $s_0 \geq 1.2511$. Here, $s_0$ is defined in units of b, i.e. $s_0$ is $s_0/b$. This function is defined for negative (the overlap region), zero (touching configuration) and positive values of $s_0$. For a fixed R, the minimum distance $s_0$ for spherical nuclei is defined as

$$s_0 = R - R_1 - R_2 \tag{2.40}$$

where $R = 1.07A_i^{1/3}(i=1,2)$. b is the diffuseness of the nuclear surface given by

$$b=[\pi/2\sqrt{3}\ln 9]\, t_{10\text{-}90} \tag{2.41}$$

where $t_{10\text{-}90}$ is the thickness of the surface in which the density profile changes from 90% to 10%. The value of b ~1 fm. The γ is the specific nuclear surface tension given by

$$\gamma = 0.9517[1-1.7826(N-Z/A)^2] \text{ Mev fm}^{-2} \tag{2.42}$$

R' is the mean curvature radius of the reaction partners, characterizing the gap, which for spherical nuclei is given by

$$\overline{R} = R_1R_2 / R_1 + R_2 \tag{2.43}$$

### 2.3.4 The Coulomb potential

Coulomb potential describes the force of repulsion between two interacting nuclei due to their charges. It acts along the line joining the two nuclei. The Coulomb potential for two interacting spherical nuclei is given as

$$V_c = Z_1Z_2e^2/ R \tag{2.44}$$

For interacting deformed and oriented nuclei, different authors [54]-[58] have derived it differently. In this thesis work, we have started with Coulomb potential of Wong [57], given for two non-overlapping charge distributions, having qudarupole deformations only, i.e.,

$$V_c = \frac{Z_1 Z_2 e^2}{R} + \left(\frac{9}{20\pi}\right)^{1/2}\left(\frac{Z_1 Z_2 e^2}{R^3}\right)\sum_{i=1}^{2} R_i^2(\alpha_i)\beta_{2i}P_2(cos\theta_i) + \left(\frac{3}{7\pi}\right)\left(\frac{Z_1 Z_2 e^2}{R^3}\right)\sum_{i=1}^{2} R_i^2(\alpha_i)\left[\beta_{2i}P_2(cos\theta_i)\right]^2 \tag{2.45}$$

In this expression, the quadrupole-quadrupole interaction term, proportional to $\beta_{21}\beta_{22}$, is neglected since it has a short-range character. For nuclei lying in the same plane we have generalized it to include the higher order deformations (λ = 3, 4...), obtaining

$$V_c(Z_i,\beta_{\lambda i},\theta_i,T) = \frac{Z_1 Z_2 e^2}{R(T)} + 3Z_1 Z_2 e^2 \sum_{\lambda,i=1,2} \frac{R_i^{\lambda}(d_i,T)}{(2\lambda+1)R(T)^{\lambda+1}} \left[\beta_{\lambda i} + \beta^2_{\lambda i} Y_{\lambda}^{(0)}(\theta_i)\right] \quad (2.46)$$

With $R_i$ from eq (2.32 ) $Y_{\lambda}^{(0)}(\Theta_i)$ are the spherical harmonic function.

## 2.3.5 Rotational Energy due to angular momentum

The rotational motion gives an additional energy due to the angular momentum define as

$$V_l = \frac{\hbar^2 l(l+1)}{8\pi^2 I} \quad (2.47)$$

with $I = \mu R^2$, is the non-sticking limit of moment of inertia with as the $\mu = \frac{A1A2}{A1+A2} m$ reduced mass. m is the nucleon mass. In the complete sticking limit, the moment of inertia I is given as,

$$I = \mu R^2 + 2/5 A_1 m R_1^2 + 2/5 A_2 m R_2^2 \quad (2.48)$$

with $R_i$ from Eq. (2.32). However, for the relative separation of interest here, we use the sticking limit. It is relevant to mention here that value of angular momentum extracted experimentally, is based upon moment of interia limit .[59]

## 2.3.6 Classical Hydrodynamical Mass Parameters

The kinetic energy part of the Hamiltonian in Eq. (2.26) enters through the mass parameters. We use here the classical mass parameters of Kroger and Scheid [47]. The model of Kroger and Scheid is based on the hydrodynamical flow, as shown in Fig. 2.3.

This model gives a simple analytical expression, whose predictions are shown to compare nicely with the microscopic cranking model calculations. For the $B_{\eta\,\eta}$ mass we get

$$B\eta\,\eta = \frac{AmR2}{4}\left[\frac{vt(1+\gamma)}{vc1+\left(\frac{vt(1+\gamma)}{vc(1+\_\delta 2)}\right)} - 1\right] \qquad (2.49)$$

With $\gamma = = \frac{Rc}{2R}\left[\frac{1}{1+\cos\vartheta 1}\left(1-\frac{Rc}{R1}\right)+\frac{1}{1+\cos\vartheta 2}\left(1-\frac{Rc}{R2}\right)\right]$ (2.50)

$$\delta = \frac{1}{2R}[(1-\cos\vartheta_1)+(1-\cos\vartheta_2)] \qquad (2.51)$$

$$v_c = \pi^2 R^2{}_c R \qquad (2.52)$$

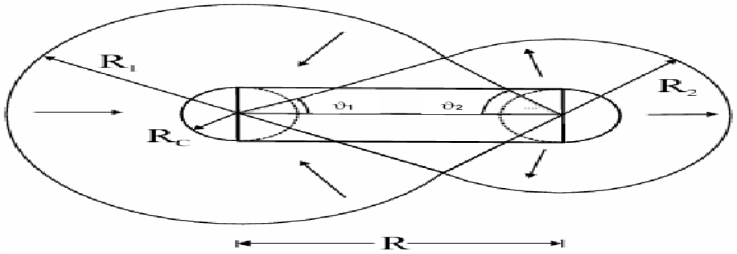


Fig 2.3 The geometry of classical hydrodynamical model for calculating mass parameter $B_{\eta\eta}$

and $v_t = v_1+v_2$, is the total conserved volume. The angles $\vartheta_1$ and $\vartheta_2$ and geometry of the model are shown in Fig. 2.3. For $\vartheta_1 = \vartheta_2 = 0$, $\delta = 0$ which corresponds to two touching spheres. $R_c$(is not equal to 0) is the radius of a cylinder of length R, having a homogeneous flow in it; whose existence is assumed for the mass transfer between the two spherical fragments. We have generalized this formalism for deformed nuclei by using the radii $R_1$ and $R_2$ for deformed nuclei, given by Eq. (2.32).

## 2.3.7 Solution of the Schrödinger Equation and the fragments preformation Probability $P_0$

Once the Hamiltonian Eq. (2.25) is established, the Schrödinger equation in mass fragmentation co-ordinate η can be solved. On solving Eq. (2.26) numerically, $|\psi^{v}(\eta)|^2$ gives the probability $P_0$ of finding the mass fragmentation η at a fixed R on the decay path.

$$P_0(A_2)=|\psi^{v}(A_2)|^2 \tag{2.53}$$

For fission studies, like the spontaneous fission and fission through the barrier, the motion in R at the saddle point is adiabatically slow as compared to the η motion.Therefore, the potential is minimized in the neck and deformation coordinates $ß_1$ and $ß_2$ at each R and η values. Starting from the nuclear ground state in spontaneous fission or cluster decay, and to have complete adiabaticity, only the lowest vibrational state $\nu = 0$ is occupied. Then, the mass (or charge) distribution yield, proportional to the probability $|\psi^{(0)}(\eta)|^2$ or $|\psi^{(0)}(\eta_z)|^2$ of finding a certain mass (or charge) fragmentation η (or $\eta_z$) at a position R on the decay path, when scaled to, say,mass $A_2$ of one of the fragments ($d\eta = 2/A$) is given by:

$$Y(A_2) = |\psi_R^{(0)}(A_2)|^2 \frac{2}{A}\sqrt{B_{\eta\eta}(A_2)}). \tag{2.54}$$

However, if the system is excited or we allow interaction between various degrees of freedom, higher values of $\nu$ would also contribute. These enter via the excitation of higher vibrational states, and through the temperature dependent potential V and masses $B_{ij}$ The effect of adding temperature on potential V and masses $B_{ij}$ is to reduce the shell effects in them, resulting finally in the liquid drop potential $V_{LDM}$ and smoothed (averaged) masses $B_{ij}$ for the systems to be very hot. Apparently, cold fission means taking both the potential V and masses $B_{ij}$ with full shell effects included in them and hot fission means using the $V_{LDM}$ and smoothed (averaged) masses $B_{ij}$ . The possible consequence of such excitations are included here by assuming a Boltzmann like occupation of excited states

$$|\psi(\eta)|^2 = \sum_{\nu=0}^{\infty} |\psi^{\nu}(\eta)|^2 \exp\left(-\frac{E_{\eta}^{\nu}}{T}\right) \tag{2.55}$$

Note that we are dealing here with a directly measurable quantity, the mass (or charge) asymmetry, which works dynamically as mass (or charge) transfer coordinate. Thus, the calculated yields Y ($A_i$) (or Y ($Z_i$)) are directly comparable with experiments. It may be stressed that there is no free parameter in these calculations. The nuclear shape, once minimized in the neck and deformation coordinates $ß_1$ and $ß_2$ at a given R (=$R_{saddle}$), remains fixed for both the mass and charge distributions of fission or decay fragments.

## 2.4 Penetration Probability P

Penetrability P measures the of capability of fragments nucleus to penetrate the potential barrier generalized during compound nucleus formation.

## 2.5 Assault Frequency $υ_0$

For the cluster decay studies in the following section, another quantity of interest is the assault frequency $υ_0$ defined as,

$$υ_0 = \frac{v}{R0} = \frac{\sqrt{(2E_2/\mu)}}{R0} \tag{2.56}$$

where $R_0$ is the radius of parent nucleus and $E_2 = 1/2\mu v^2$ is the kinetic energy of the emitted cluster. Since both the emitted cluster and the daughter nucleus are produced in the ground state, the entire positive Q-value is the total kinetic energy ($Q = E_1 + E_2$) available for the decay process, which is shared between two fragments, such that for the emitted cluster

$$E_2 = \left(\frac{A_1}{A}\right)Q \tag{2.57}$$

and, $E_1 = Q - E_2$ is the recoil energy of the daughter nucleus.

## 2.6 References


[1] R.K. Gupta, M. Balasubraniam, C. Mazzocchi, M. La Commara, and W. Scheid, Phys. Rev. C 65, 024601 (2002).

[2] M.K. Sharma, R.K. Gupta, and W. Scheid, J. Phys. G 26, L45 (2000).

[3] R.K. Gupta, R. Kumar, N.K. Dhiman, M. Balasubraniam, W. Scheid, and C. Beck, Phys. Rev. C 68, 014610 (2003).

[4] M. Balasubraniam, R. Kumar, R.K. Gupta, C. Beck, and W. Scheid, J. Phys. G 29, 2703 (2003): R.K. Gupta, M.K. Sharma and B. Singh, Phys. Rev. C-to be published

[5] R.K. Gupta, M. Balasubraniam, R. Kumar, D. Singh, and C. Beck, Nucl. Phys. A 738, 479c (2004).

[6] R.K. Gupta, M. Balasubramaniam, R. Kumar, D. Singh, C. Beck, and W. Greiner, Phys. Rev. C 71, 014601 (2005).

[7] B.B. Singh, M.K. Sharma, R.K. Gupta, and W.Greiner,Int.J. Mod.Phys.E15, 699 (2006)

[8] R.K. Gupta, M. Balasubraniam, R.Kumar, D.Singh ,S. K. Arun and W.Greiner,J.Phys .G:Nucl.Part. Phys. 32, 345(2006)

[9] B.B. Singh, M.K. Sharma, R.K. Gupta,Phys.Rev. C 77, 054613 (2008)

[10] R.Gupta, in proceedings of the 5$^{th}$ International Conference on Nuclear Research Mechanics, Varenna, 1988, edited by E. gladioli , (Ricerca Scientifica ed Educazione Permanente ,Milano, 1988),p.416.

[11] S.S. Malik and R.K.Gupta, Phys.Rev.C 39, 1992(1989)

[12] R.K.Gupta, W.Scheid, and W.Greiner, J.Phys.G:Nucl. Part. Phys. 17, 1731(1991).

[13] S. Kumar and R.K.Gupta, Phys.Rev. C 49, 1922(1994).

[14] R.K.Gupta and W. Greiner Int. J. Mod. Phys. E 3, 335 (1994, Suppl.).

[15] S. Kumar and R.K.Gupta, Phys. Rev. C 55, 218 (1997).

[16] R.K. Gupta, in Heavy Elements and Related New Phenomena ,edited by W.Greneir and R.K Gupta (World Scientific Singapore ) Vol.II ,p.730

[17] S.K and R.K Gupta ,DAE nucl.Phys.(Sambalpur )52,365(2007)

[18] B.B.Singh,S.K Arun, M.K.Sharma , S.Kanwar and Raj K.Gupta ,DAE Nucl.Phys.(Roorkee), Accepted(2008)

[19] J. Maruhn and W. Greiner, Phys. Rev. Lett. 32, 548 (1974).

[20] R.K. Gupta, W. Scheid and W. Greiner, Phys. Rev. Lett. 35, 353 (1975).

[21] A. S¡andulescu, R.K. Gupta, W. Scheid and W. Greiner, Phys. Lett. 60B, 225 (1976).

[22] R.K. Gupta, A. S¡andulescu and W. Greiner, Phys. Lett. 67B, 257 (1977); Rev. Roum. Phys. 23, 51 (1978).

[23] S. Yamaji, W. Scheid, H.J. Fink and W. Greiner, Z. Phys. A 278, 69 (1976).

[24] S. Yamaji, W. Scheid, H.J. Fink and W. Greiner, J. Phys. G: Nucl. Phys. 2, L189 (1976).

[25] S. Yamaji, K.H. Ziegenhain, H.J. Fink, W. Greiner and W. Scheid, J. Phys. G: Nucl. Phys. 3, 1283 (1977).

[26] R.K. Gupta, A. S¡andulescu and W. Greiner, Z. Naturforsch. 32a, 704 (1977).

[27] R.K. Gupta, C. Pirvulescu, A. S¡andulescu and W. Greiner, Z. Phys. A 283, 217 (1977); Sovt. J. Nucl. Phys. 28, 160 (1978).

[28] R.K. Gupta, Z. Physik. A 281, 159 (1977).

[29] A. S¡andulescu, H.J. Lustig, J. Hahn, and W. Greiner, J. Phys. G: Nucl. Phys.4, L279 (1978).

[30] H.J. Lustig, J.A. Maruhn, and W. Greiner, J. Phys. G: Nucl. Phys. 6, L25

(1980).

[31] H.J. Fink and W. Greiner and R.K. Gupta and S. Liran and J.H. Maruhn and W. Scheid and O. Zohni, in Proceedings of Int. Conf. on Reaction between Complex Nuclei, Nashville, 1974, 21, (Amsterdam: North Holland), pages 2.

[32] R. K. Gupta, IANCAS Bull. (India), 6, 2(1990).

[33] R.K. Gupta, N.Singh, and M. Manhas, Phys. Rev. C 70, 034608 (2004)

[34] R.K. Gupta ,M.balasubramaniam, R.Kumar, N.Singh, M.Manhas, and W. Greiner, J.Phjs. G: Nucl.Part. Phys. C 31, 631(2005).

[35] T. Matsuse, C. Beck, R. Nouicer, and D. Mahboub, Phys. Rev. C 55, 1380 (1997).

[36] S.J. Sanders, D.G. Kovar, B.B. Back, C. Beck, D.J. Henderson, R.V.F. Janssens, T.F. Wang, and B.D. Wilkins, Phys. Rev. C 40, 2091 (1989t).

[37] S.J. Sanders, Phys. Rev. C 44, 2676 (1991).

[38] J. Gomez del Campo, R.L. Auble, J.R. Beene, M.L. Halbert, H.J. Kim, A. D'Onofrio, and J.L. Charvet, Phys. Rev. C 43, 2689 (1991); Phys. Rev. Lett. 61, 290 (1988).

[39] R.J. Charity, M.A. McMahan, G.J. Wozniak, R.J. McDonald, L. G. Moretto, D.G. Sarantites, L.G. Sobotka, G. Guarino, A. Pantaleo, L. Fiore, A. Gobbi and K.D. Hildenbrand, Nucl. Phys. A 483, 371 (1988).

[40] C. Beck, R. Nouicer, D. Disdier, G. Duchˆene, G. de France, R.M. Freeman, F. Haas, A. Hachem, D. Mahboub, V. Rauch, M. Rousseau, S.J. Sanders, and A. Szanto de Toledo, Phys. Rev. C 63, 014607 (2001).

[41] N.J. Davidson, S.S. Hsiao, J. Markram, H.G. Miller, and Y. Tzeng, Nucl. Phys. A 570, 61c (1994).

[42] G. Audi and A.H. Wapstra, Nucl. Phys. A 595, 4 (1995).

[43] G. Audi and A.H. Wapstra and C. Thiboult, Nucl. Phys. A 729, 337(2003)

[44] P. M¨oller, J. R. Nix, W. D. Myers, and W. J. Swiatecki, At. Data Nucl. Data Tables 59, 185 (1995).

[45] W. Myers and W.J. Swiatecki, Nucl. Phys. 81, 1 (1966).

[46] P. A.Seeger, Nucl. Phys. 25, 1 (1961)

[47]H.Kroger and W. Scheid, J. Phys. G 6, L85(1980)

[48] S.J. Sanders, D.G. Kovar, B.B. Back, C. Beck, B.K. Dichter, D. Henderson, R.V.F. Janssens, J.G. Keller, S. Kaufman, T.-F. Wang, B. Wilkins, and F. Videbaek, Phys. Rev. Lett. 59, 2856 (1987).

[49] V.M. Strutinsky, Nucl. Phys. A 95, 420 (1967).

[50] J. Blocki, J. Randrup, W. J. Swiatecki, and C. F. Tsang, Ann. Phys. (NY) 105, 427 (1977).

[51] Deryagin, Kolloid Z. 69, 155 (1934).

[52] A. Gray, Modern Di_erential Geometry of Curves and Surfaces with Mathematica, 2nd Edition, CRC Press, Boca Raton, 1997, p.89.

[53] M. Seiwert, W. Greiner, V. Oberacker, and M.J. Rhoades-Brown, Phys. Rev. C 29, 477 (1984).

[54] N. Malhotra and R.K. Gupta, Phys. Rev. C 31, 1179 (1985).

[55] M M¨unchow, D Hahn and W Scheid, Nucl. Phys. A 388, 381 (1982).

[56] M J Rhoades-Brown, V E Oberacker, M Seiwert and W Greiner, Z. Phys. A 310, 287 (1983).

[57] C Y Wong, Phys. Rev. Lett. 31, 766 (1973).

[58] R Aroumougame and R K Gupta, J. Phys. G: 6, L155 (1980).

[59]S.Kailais(private communication)

# Chapter 3

## *3.1 Observation and Calculations*

In order to investigate the possible role of deformation and orientation in the decay of heavy nuclei in the mass region A~200 we have chosen the recent experiment on $^{132}Sn+^{64}Ni\rightarrow^{196}Pt$ reaction. Since this reaction is an inverse kinematics. (a heavy projectile on a light target). So it extends a decent case for investigating nuclear dynamics and related properties. In this reaction fission cross-sections are negligible for $E_{c.m.} \leq 160$ Mev, so the evaporation residue cross sections are taken as fusion cross sections.

The Fusion – Evaporation Cross Section for the reaction $^{132}Sn+^{64}Ni\rightarrow ^{196}Pt$ have been measured [1] at various $E_{c.m.}$ $^{132}Sn$ is spherical nuclei. which means that $\beta_2$ and $\beta_4$ for the $^{132}Sn$ is zero. For $^{64}Ni$ $\beta_2$ (quadrupole deformation) ,$\beta_4$ (hexadecapole deformation) = - 0.087 and -0.005 respectively. And for $^{196}Pt$ $\beta_2$ , $\beta_4$ = -0.139 and -0.030 respectively. The decay of Compound nucleus $^{196}Pt$ formed in $^{132}Sn+^{64}Ni$ reaction is studied by explicitly incorporating the deformation & orientation using DCM [2-10] contributions in the decay process of chosen nuclear system.

In order to investigate the role of deformations in the decay of $^{196}Pt$ formed in heavy ion reaction we have also done calculations in the spherical considerations as well. For deformed considerations we have takn quadrupole deformations for i.e. for $\beta_2$ alone. Our calculations predict that experimental data can be reproduced only with the deformed fragment considerations. As expected the barrier height is much lower for the deformed case as compared to spherical considerations.

### *3.2 . Results and discussions*

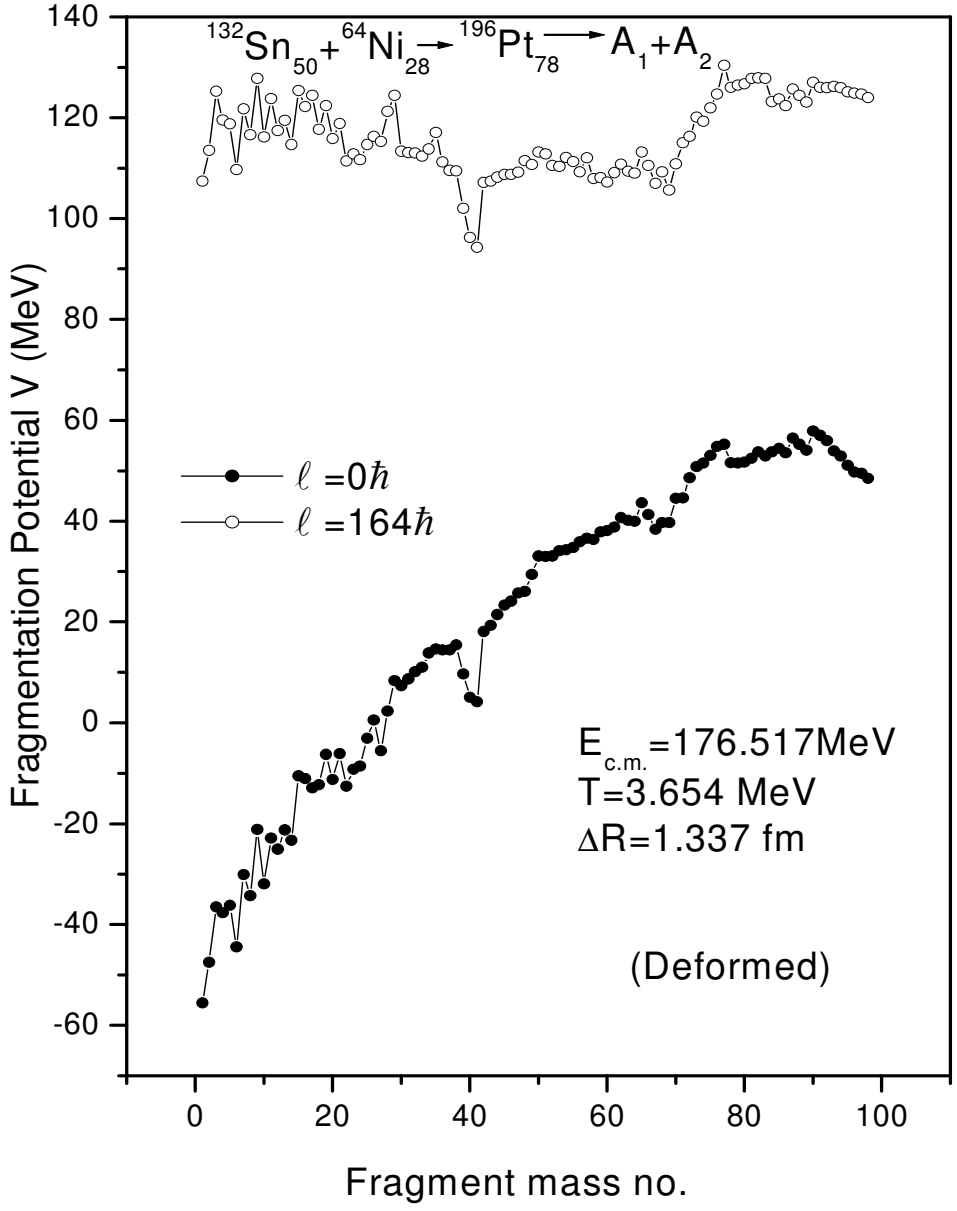


Fig 3.1 The fragmentation potential as a function of the light fragment mass $A_2$ formation of $^{196}Pt$ at $E_{c.m.}$ =176.517MeV, calculated at two extreme $\ell$ values.

Figure 3.1 shows the calculate fragmentation potential for the decay of compound nucleus $^{196}$Pt (at $E_{c.m.}$ =176.517MeV or T = 3.654MeV) for two extreme cases of $\ell$ – values ($\ell$ = 0 & $\ell$ = $\ell_{max}$); using quadrupole deformations ($\beta_2$). A minima is observed in fragmentation potential both for $\ell$ =0 and $\ell$ =164 for fragment A= 40. but for $\ell$ =0 the

fragmentation potential is approximately increasing with increase in fragment mass number except for fragment A= 40. The α- nuclear structure is evident even at temperature as high as 3.6 MeV. Clearly ER contributions is more favorable as compared to fission fragments. At higher $\ell$ –values as well the α – nuclear structure is still evident however contribution of fragments is drastically changed. Here fission fragments are equally favorable as that of ERs.

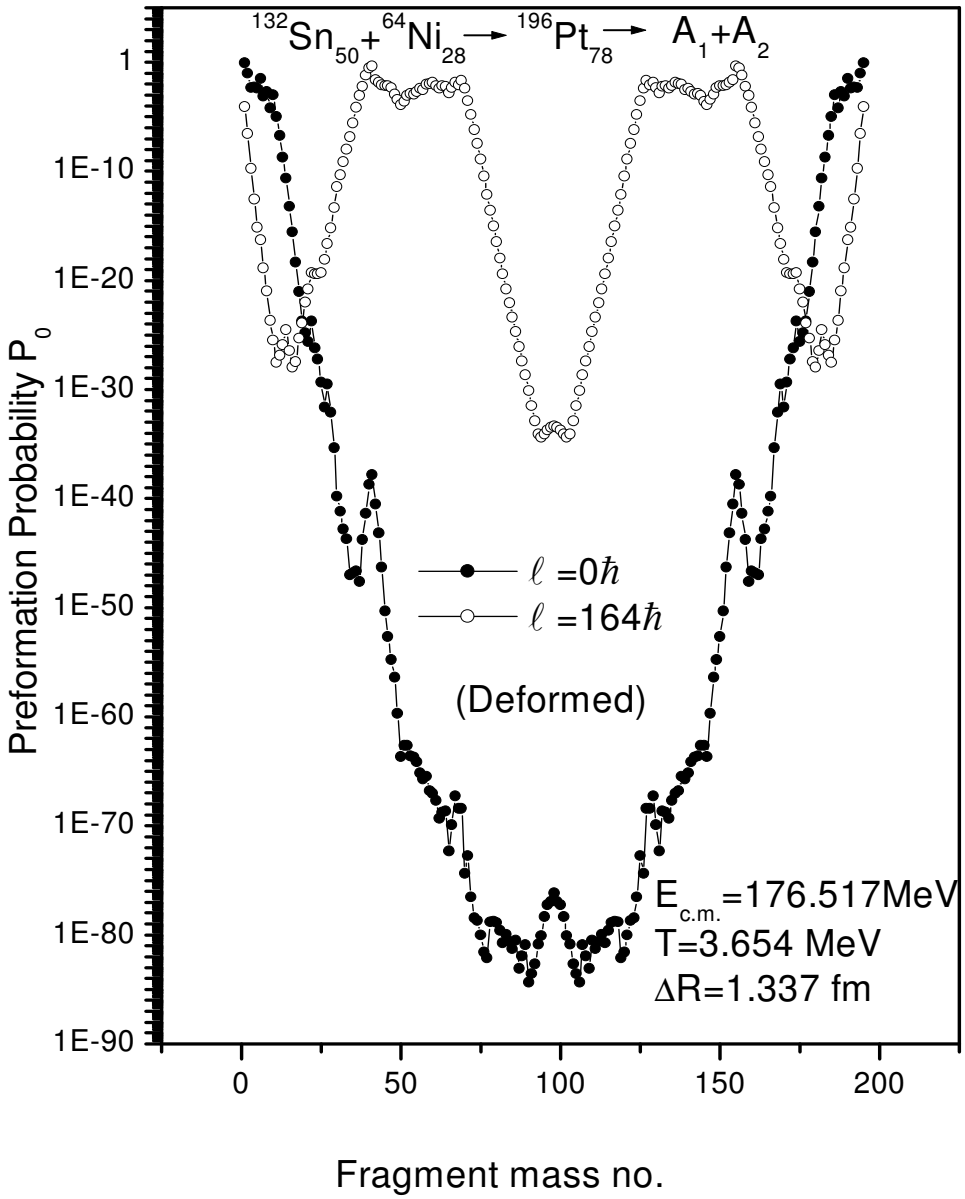


Fig 3.2. same as fig.3.1. but for preformation probability $P_0$

Figure 3.2 shows the preformation probability $P_0$ at $\ell$ = 0 and $\ell_{max}$ it is found that minima in the fragmentation potential of fig. 3.1 act as a maximum in the preformation probability. The change of behavior as discussed in fig. 3.1 is again evident in fig. 3.2. Here also at $\ell$ =0 ER is prominent as compared to fission and at $\ell = \ell_{max}$ asymmetric fission becomes comparable to ERs.

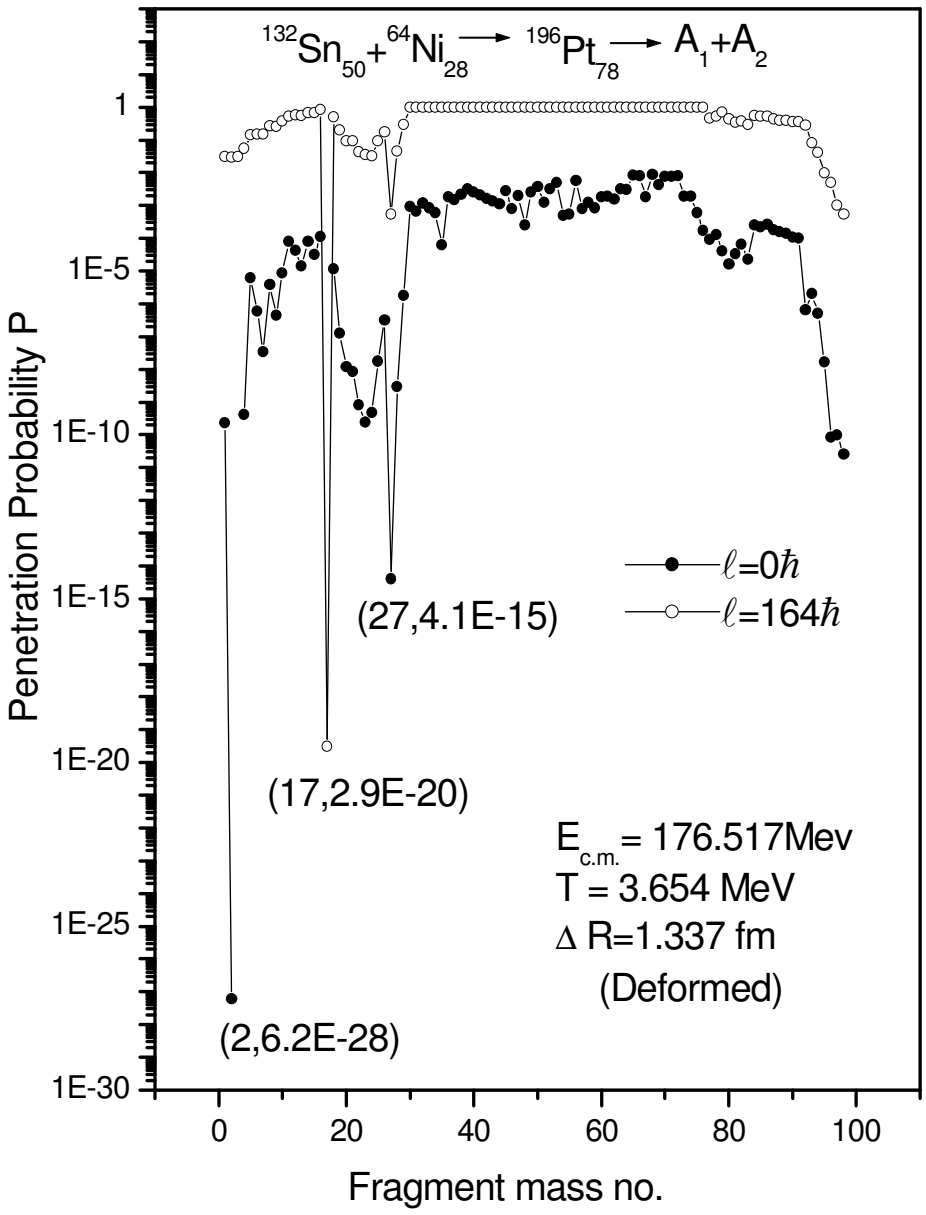


Fig.3.3 Same as fig. 3.1, but for penetration probability.

In fig. 3.3, we find some structure at $\ell = 0$ where as at $\ell = \ell_{max}$ Penetrability approaches maximum value i.e. P ~1 for majority of cases. This result plays significant role in drawing comparison with available experimental data. There are certain down

peaks at $A_2$ = 27,17,2. These minimas indicate that these fragments are not favored on the basis of penetration criteria.

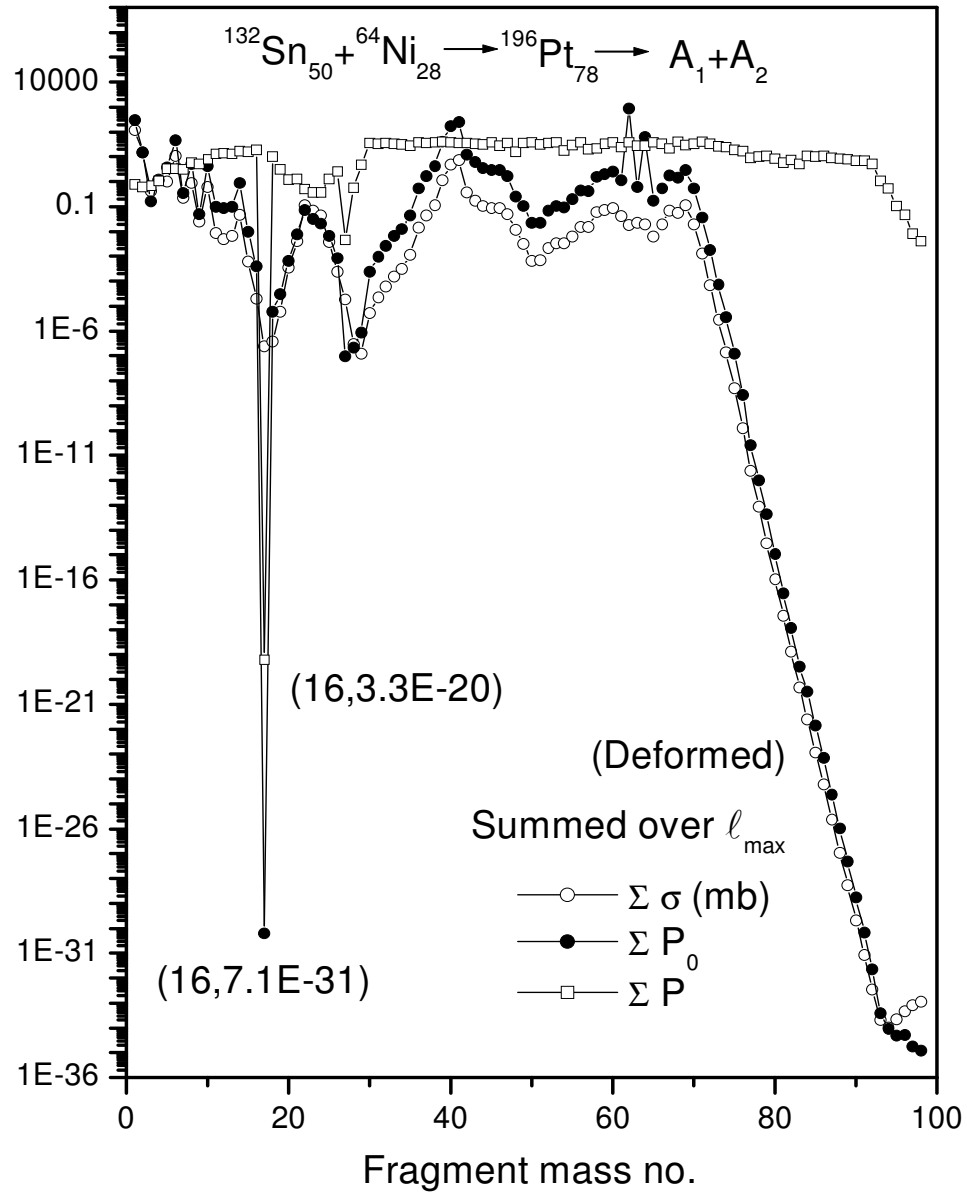


Figure.3.4. variation of summed cross section ,P, $P_0$ over $\ell_{max}$ with fragment mass number.

Fig.3.4 represents the calculated cross section (σ), Penetrability(P), Preformation probability($P_0$) as a function of fragment mass no. summed over $\ell_{max.}$ Fig.3.4. clearly depict that Preformation probability $P_0$ shows an interesting structure as that for cross-section(σ), where as on the other hand, Penetrability P plays a silent role atleast on structure front and contributes only in magnitude.

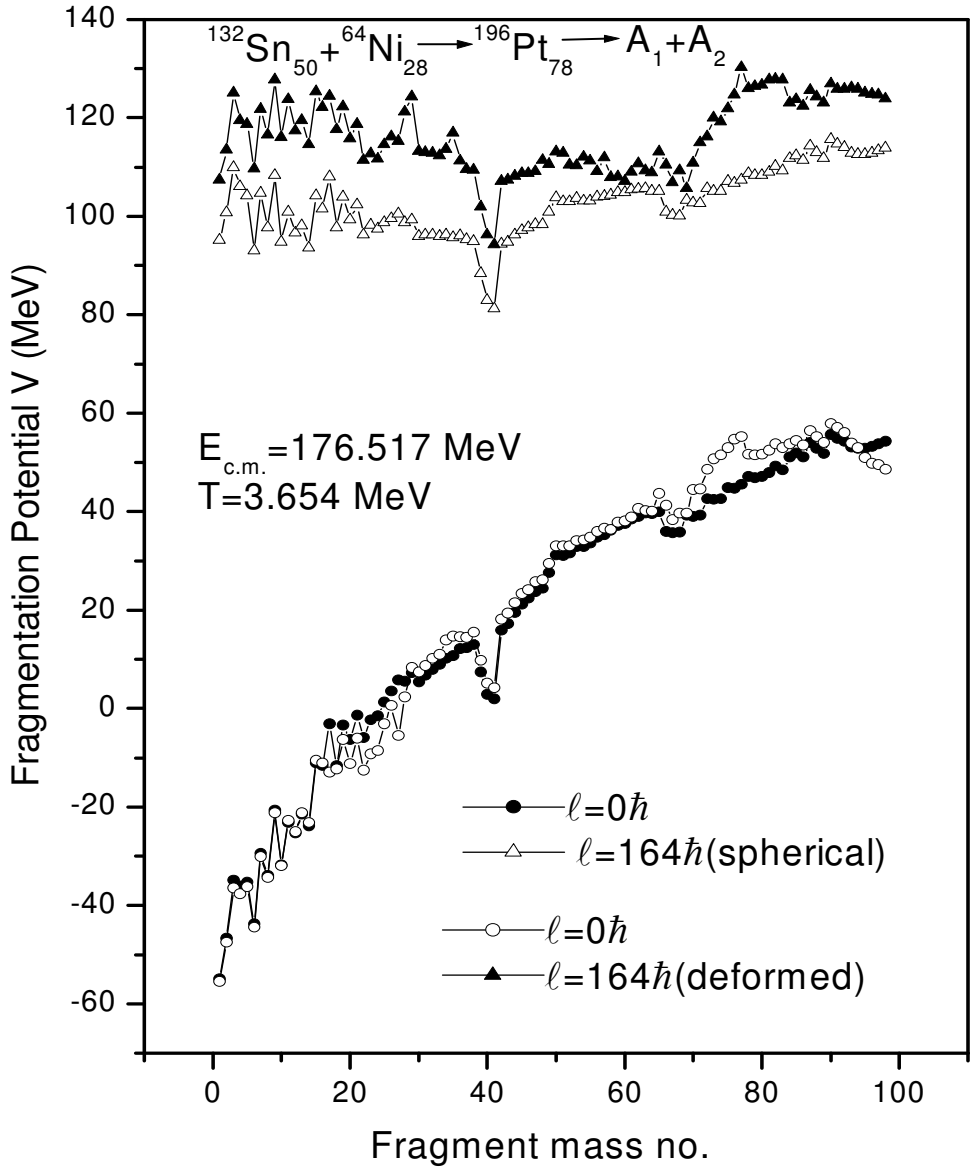


Figure 3.5. fragmentation potential versus fragment mass no. for spherical as well as for deformed nuclei.

Fig 3.5. shows the comparison between spherical and deformed consideration for the decay of $^{196}$Pt nuclear system formed in $^{132}$Sn+$^{64}$Ni reaction. The fragmentation potential clearly indicate that deformation play significant role at $\ell = \ell_{max}$. It is relevant to mention here that we have tried to fit the experimental data with spherical consideration as well but without much success except at couple of energies. Therefore the incorporation of deformation & orientation effects become obvious at least for this reverse kinematics reaction in the energy range ~ 142-176 MeV .

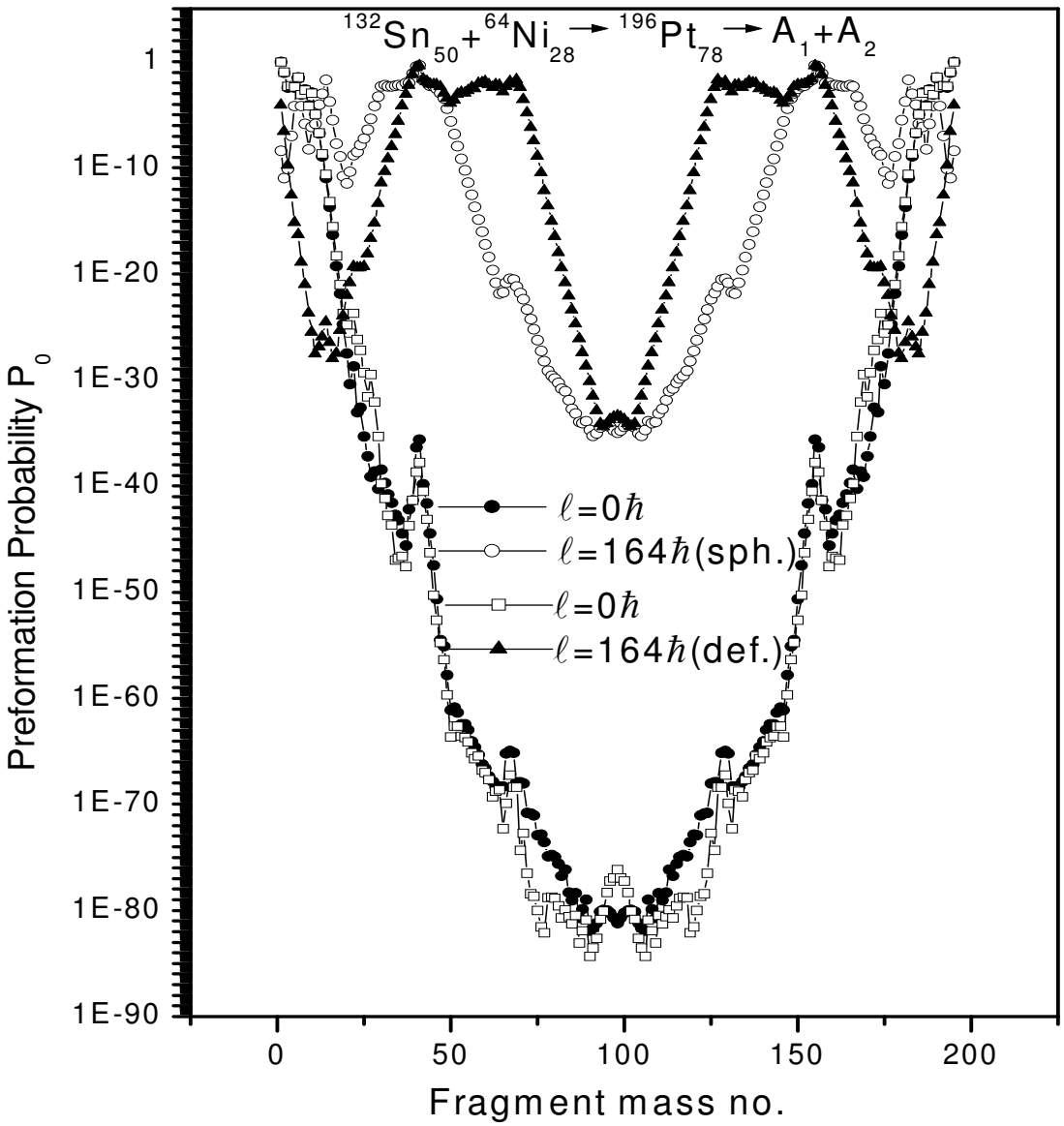


Figure 3.6. Preformation probability for spherical as well as deformed nuclei.

Fig. 3.6. shows the variation of $P_0$ for spherical and deformed nuclei at $\ell = 0$ & $\ell = \ell_{max}$..

For $\ell = 0$ the variation is quite similar for spherical and deformed consideration. However the role of deformations & orientations becomes evident at $\ell = \ell_{max}$ case.

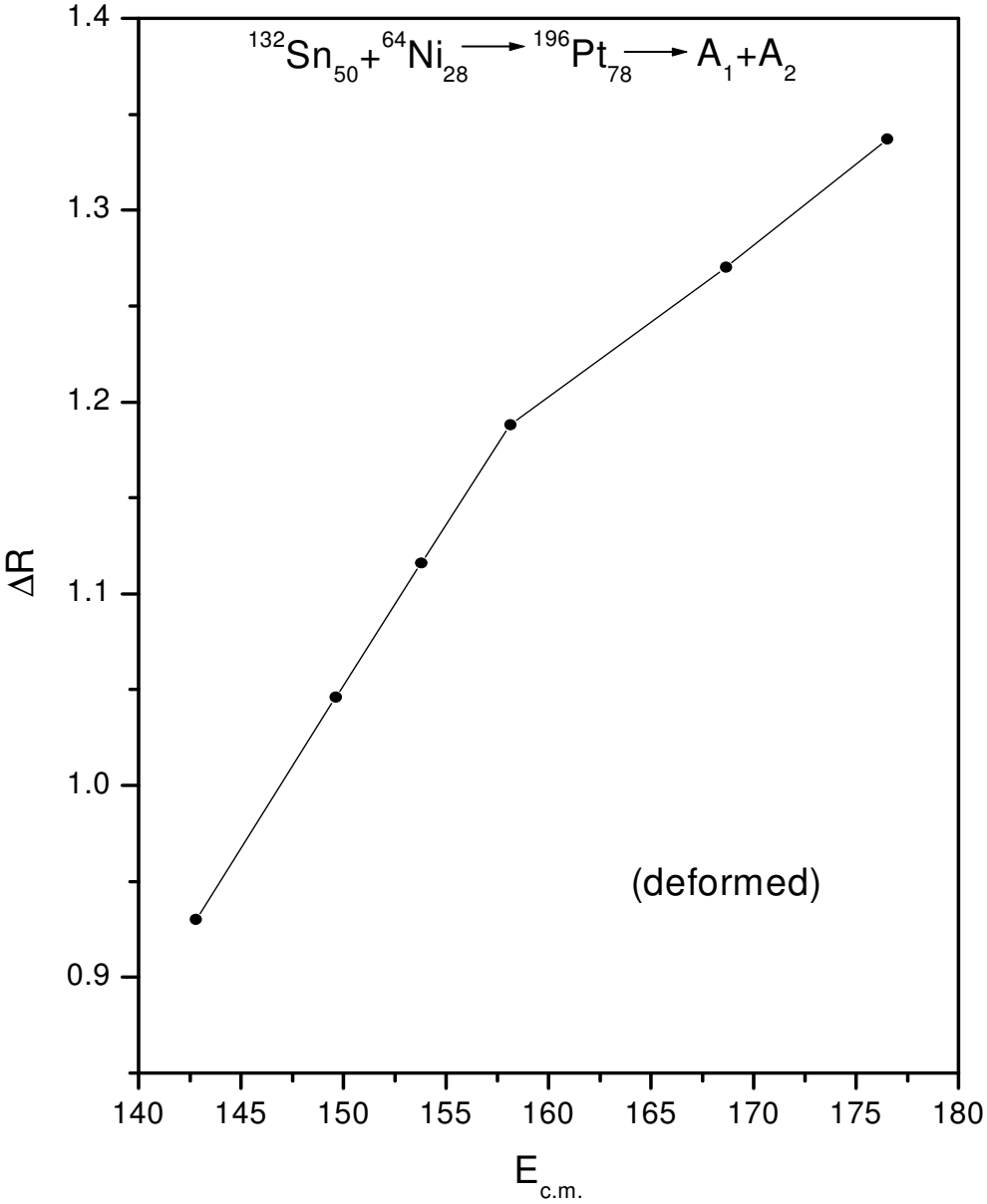


Figure.3.7. DCM calculated cross-section for deformed consideration along in the experimental data[1].

Fig.3.7. gives a comparison of our DCM calculated Evaporation fusion cross section for spherical and deformed nuclei at different centre of mass energies With the experimental data. It is clearly evident that DCM calculated cross-sections for deformed choice of fragments find an excellent comparison with experimental data at all reported $E_{c.m.}$ values.

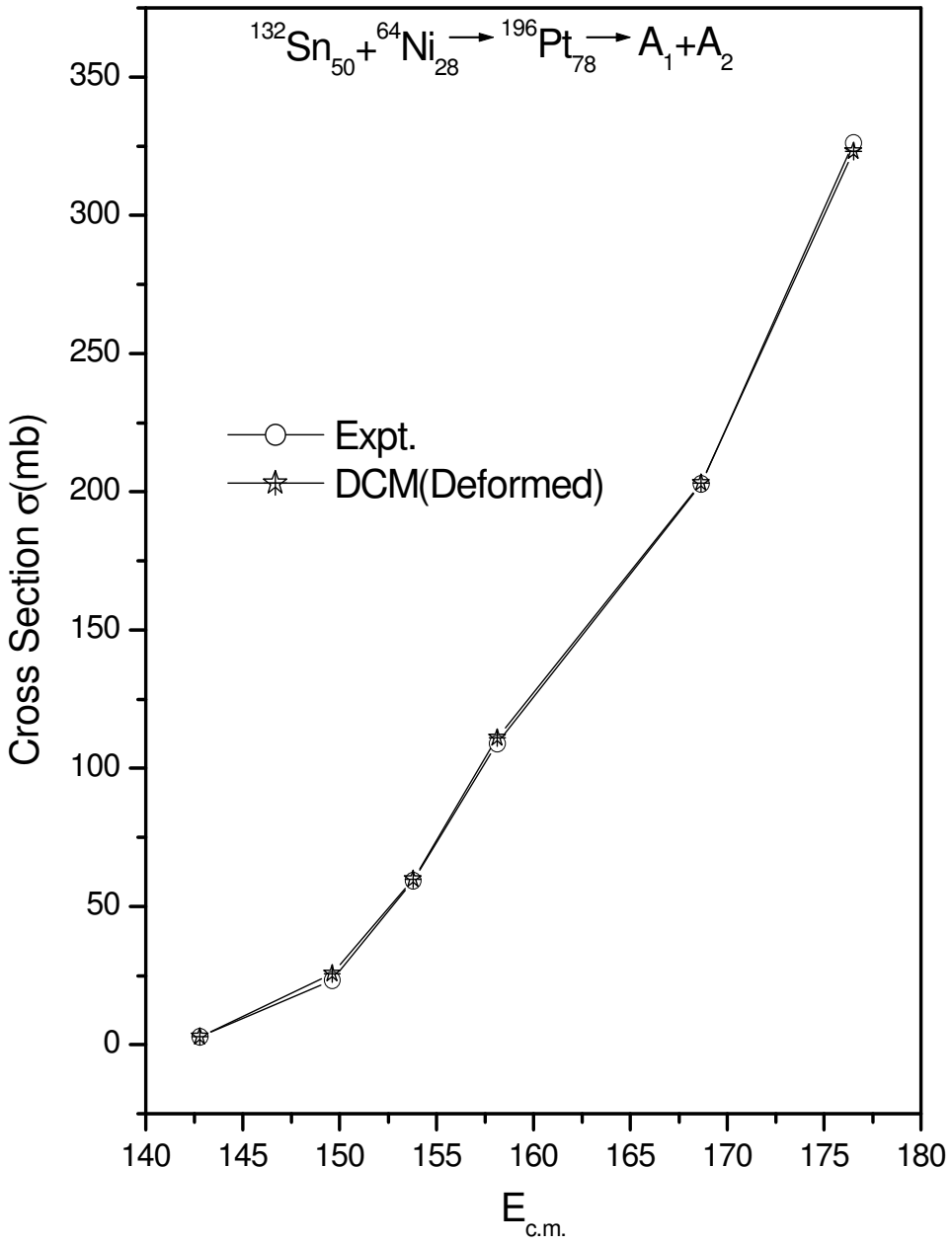


Figure.3.8 ΔR versus $E_{c.m.}$ for deformed nuclei.

Fig.3.8. shows that the variation of ΔR with $E_{c.m.}$ it shows that ΔR increases almost linearly with increase in $E_{c.m.}$ values. Because of the linear dependence of ΔR on $E_{c.m.}$ it becomes possible to extrapolate the value of ΔR at higher and lower $E_{c.m.}$

Table 3.1:

| Temp. (MeV) | $E_{c.m}$ (Mev) | $\Delta$R(fm) | DCM (deformed) | Experimental σ |
|---|---|---|---|---|
| 3.65384 | 176.517 | 1.337 | 323.0 | 326.1224 |
| 3.6038 | 168.660 | 1.27 | 203.0 | 202.8267 |
| 3.5357 | 158.147 | 1.188 | 111.0 | 108.8566 |
| 3.5072 | 153.790 | 1.116 | 59.9 | 59.423 |
| 3.480 | 149.633 | 1.046 | 23.3 | 23.3641 |
| 3.4339 | 142.798 | 0.93 | 2.76 | 2.96396 |

The results are summarized in table 3.1. The $\Delta R$ values increase almost linearly as a function of $E_{c.m}$. The DCM calculated cross-section for ER using quadrupole deformation ($\beta_2$ only) at optimum orientations show nice comparison with available experimental data & hence predictions made regarding the fragmentation of $^{196}$Pt are useful.

## 3.3 References


[1] J.F. Liang, D. Shipra, C.J. Gross , PhysRevLett.91.152701 (2003).

[2] R.K. Gupta, M. Balasubraniam, C. Mazzocchi, M. La Commara, and W. Scheid, Phys. Rev. C 65, 024601 (2002).

[3] M.K. Sharma, R.K. Gupta, and W. Scheid, J. Phys. G 26, L45 (2000).

[4] R.K. Gupta, R. Kumar, N.K. Dhiman, M. Balasubraniam, W. Scheid, and C. Beck, Phys. Rev. C 68, 014610 (2003).

[5] R.K. Gupta, W. Scheid and W. Greiner, Phys. Rev. Lett. 35, 353 (1975).

[6] R. K. Gupta, IANCAS Bull. (India), 6, 2(1990).

[7] R.K. Gupta, N.Singh, and M. Manhas, Phys. Rev. C 70, 034608 (2004)

[8] R.K. Gupta ,M.balasubramaniam, R.Kumar, N.Singh, M.Manhas, and W. Greiner, J.Phjs. G: Nucl.Part. Phys. C 31, 631(2005).

[9] S.S. Malik and R.K.Gupta, Phys.Rev.C 39, 1992(1989)

[10] R.K.Gupta, W.Scheid, and W.Greiner, J.Phys.G:Nucl. Part. Phys. 17, 1731(1991).

# Chapter 4

## *Summary*

In this thesis we have studied the decay of compound nucleus $^{196}$Pt formed in the entrance channel $^{132}$Sn + $^{64}$Ni at different centre of mass energies.The results of our DCM calculations, using deformed fragmentation are nicely compared with the experimental data. Our calculations clearly demonstrate that the calculations for deformed consideration reproduces experimental data quit successfully. On the contrary we find rather poor comparison with spherical choice of fragmentation. We have studied the possibilities of using deformed nuclei within the quantum mechanical fragmentation theory, since for a deformed combination, the barrier height is reduced significantly with respect to that for spherical target projectile nuclei. Another interesting feature of deformation effects is that the probability of fusion increase significantly with incorporation of deformation effects and hence the "island of stability" or extension the periodic table of elements dream of seen possible.

For the reaction $^{132}$Sn + $^{64}$Ni→ $^{196}$Pt the calculations are in good agreement with the experimental data for all c.m. energies in case of deformed nuclei. Note, however, that there is a parameter (the length parameter ΔR) to be fitted in this model, which shows approximate linear dependence on the c.m. energies in case of deformed nuclei. This linear dependence of ΔR on $E_{c.m.}$ can be exploited to predict nuclear cross-sections for lower and higher range of reported $E_{c.m.}$ values.

The detail of theoretical formulation is discussed in chapter 2. This includes the extended quantum mechanical fragmentation theory, extended for the use of deformed and oriented nuclei within the generalized nuclear proximity and Coulomb potentials. Finally, the solutions of the stationary Schrodinger wave equations for the coordinates of mass asymmetry and relative separation are also discussed.

Our calculations clearly indicate that at lower $\ell$ -values ER is a prominent decay process where as at higher $\ell$ -values fusion-fission becomes comparable with ER

process. Another interesting result is that preformation probability plays a significant role in deciding the cross-section of the reaction whereas Penetrability plays a silent role on structure front and contribute only towards the magnitude. We have thus seen that deformations and orientations of nuclei play a very important role in the cross sections and lowering of barrier height. Also in some of the recent experiments in nuclear physics the deformation and orientation of nuclei are very well utilized for the synthesis of super -heavy nuclei because of lowering of barrier height around the coulomb barrier for the deformed nuclei. So the deformations and orientations of nuclei play a very important role and it is believed that with deformation and orientation of nuclei one can extend the periodic table and resolve various aspects related to nuclear dynamics.